LIÈGE université Library

http://lib.uliege.be https://matheo.uliege.be

Investigating the influence of aeolian snow transport processes on the representation of the climate and surface mass balance of the Antarctic Peninsula

Auteur : Parotto, Gilles
Promoteur(s) : Amory, Charles; Fettweis, Xavier
Faculté : Faculté des Sciences
Diplôme : Master en sciences géographiques, orientation climatologie, à finalité approfondie
Année académique : 2018-2019
URI/URL : http://hdl.handle.net/2268.2/7382

Avertissement à l'attention des usagers :

Tous les documents placés en accès ouvert sur le site le site MatheO sont protégés par le droit d'auteur. Conformément aux principes énoncés par la "Budapest Open Access Initiative"(BOAI, 2002), l'utilisateur du site peut lire, télécharger, copier, transmettre, imprimer, chercher ou faire un lien vers le texte intégral de ces documents, les disséquer pour les indexer, s'en servir de données pour un logiciel, ou s'en servir à toute autre fin légale (ou prévue par la réglementation relative au droit d'auteur). Toute utilisation du document à des fins commerciales est strictement interdite.

Par ailleurs, l'utilisateur s'engage à respecter les droits moraux de l'auteur, principalement le droit à l'intégrité de l'oeuvre et le droit de paternité et ce dans toute utilisation que l'utilisateur entreprend. Ainsi, à titre d'exemple, lorsqu'il reproduira un document par extrait ou dans son intégralité, l'utilisateur citera de manière complète les sources telles que mentionnées ci-dessus. Toute utilisation non explicitement autorisée ci-avant (telle que par exemple, la modification du document ou son résumé) nécessite l'autorisation préalable et expresse des auteurs ou de leurs ayants droit.

Université de Liège
Faculté des Sciences
Département de Géographie

Investigating the influence of aeolian snow transport processes on the representation of the climate and surface mass balance of the Antarctic Peninsula

A modelling study using a high-resolution regional climate model over the period 1980-2018

Mémoire présenté par

Gilles PAROTTO

en vue de l'obtention du titre de
Master en Sciences géographiques, orientation climatologie à finalité approfondie

Année académique
2018-2019

Membres du jury:
Charles Amory (Promoteur)
Xavier Fettweis (Co-promoteur)
Aurélia Ferrari (Lectrice)

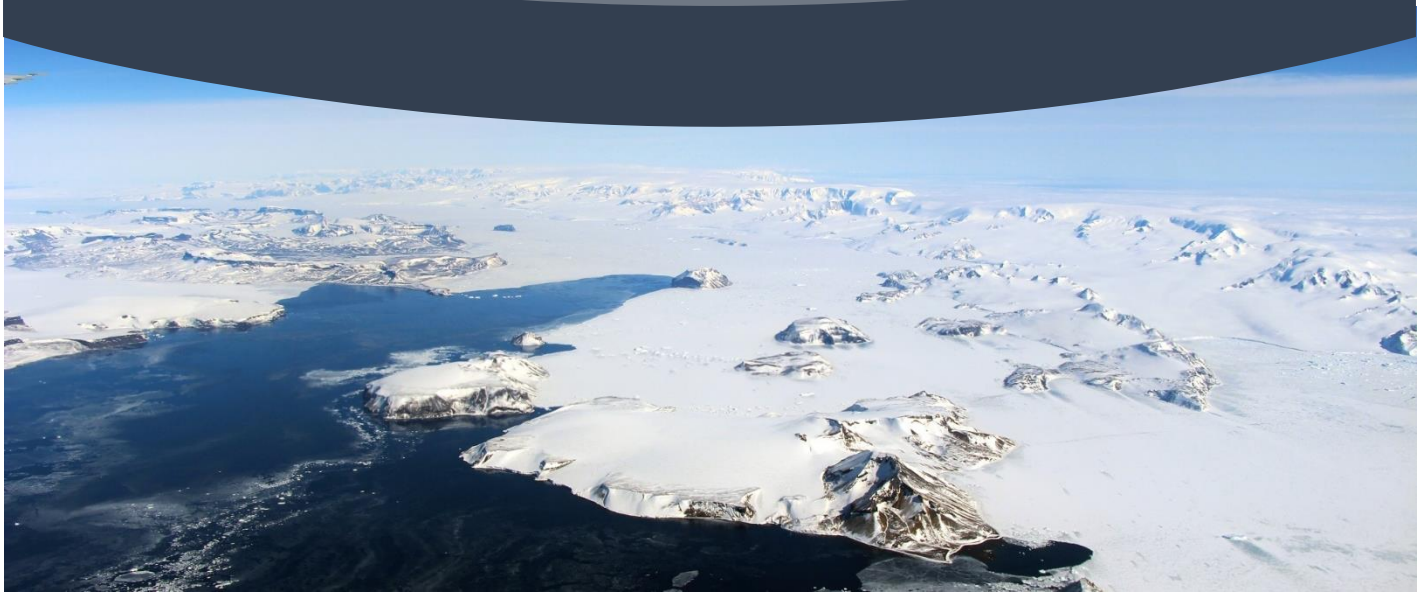

Front page picture credits: NASA/John Sonntag

ACKNOWLEDGMENTS

Je tiens tout d'abord à remercier mon promoteur principal, Charles, pour m'avoir proposé ce sujet et m'avoir accompagné avec un enthousiasme infaillible, pour ses compétences de formateur passionné et sa grande disponibilité. Un grand merci également à mon co-promoteur Xavier Fettweis pour sa confiance et son suivi, qu'il s'agisse de sa veille sur le bon déroulement technique des simulations ou plus généralement sur le fond lors de la rédaction de ce mémoire.

Un merci ne suffirait pas à Christoph pour son support, principalement sur les aspects techniques, mais aussi moral. Son soutien a été d'une importance considérable dans la réalisation de ce travail.

Je remercie également les membres du laboratoire de climatologie et autres géographes qui m'ont accueilli dans leurs bureaux, aidé ou simplement encouragé : Sébastien, Alison, Alexandre, Coraline, Charlotte, Imke et Stefan, Meriem et Myriem. Merci également à Aurélia Ferrari pour l'intérêt porté à cette étude.

Enfin, je remercie mes proches pour le soutien qu'ils et elles m'ont apporté durant mon travail et durant mes études. Merci à Mysou, Rosette, Marianne, Lorine, Lorraine, Marjorie, Alexandre, Shanti, Claire, Evelyne et Alexandra.

ABSTRACT

English

Knowledge of the evolution of the surface mass balance (SMB) of the different terrestrial ice caps is essential in estimating future sea level evolution. High-resolution regional modelling offers considerable opportunities for the study of the SMB and constantly takes more physical processes into account. One of these processes, the aeolian snow transport, contributes significantly to the mass reduction of polar ice caps and has recently been parameterized in the regional climate model MAR. For the first time, the role of this process in the representation of the climate and SMB of the Antarctic Peninsula by MAR is investigated. Here we simulate the climate and BMS of the Antarctic Peninsula at 7.5 kilometers resolution over the period 1980-2018 (38 years) using two model configurations: one without and one with the blowing snow module (BSM). The evaluation of the model is generally satisfactory with regard to climate, but MAR overestimates the SMB. The use of the BSM reduces this bias but increases some others in the representation of climate variables. Climate results show that BSM cools down the atmosphere and slightly humidifies it. Regarding the SMB, the BSM reduces surface sublimation, increases melting and re-freezing and increases, albeit to a limited extent, run-off rates. We attribute these differences mainly to the erosion-induced exposure of deeper snow layers with lower albedo, as well as changes in temperature and relative humidity of the boundary layer.

Français

La connaissance de l'évolution du bilan de masse de surface (BMS) des différentes calottes glaciaires terrestres est primordiale dans l'estimation de l'évolution future du niveau marins. La modélisation régionale à haute résolution offre des opportunités considérables pour l'étude du BSM et prend constamment davantage de processus physiques en compte. L'un de ces processus, le transport éolien de la neige, contribue de manière significative à la diminution de masse des calottes polaires et a récemment été paramétré dans le modèle climatique régional MAR. Pour la première fois, le rôle de ce processus dans la représentation du climat et du BMS de la Péninsule Antarctique par MAR est analysé. Nous simulons le climat et le BMS de la Péninsule Antarctique à 7,5 kilomètres de résolution sur la période 1980-2018 (38 ans) en utilisant deux configurations du modèle: l'une sans le module de neige aérotransportée (MNA), l'autre avec. L'évaluation du modèle est globalement satisfaisante en ce qui concerne le climat, mais MAR surestime le BMS. L'utilisation du MNA réduit ce biais mais en accroît certains autres dans la représentation des variables climatiques. Les résultats concernant le climat montrent que le MNA refroidit l'atmosphère et l'humidifie légèrement. En ce qui concerne le BMS, le MNA réduit la sublimation de surface, augmente la fonte ainsi que le regel et augmente, bien que de manière limitée, le ruissèlement. Nous attribuons ces différences principalement à l'exposition de couches de neige plus profondes avec un albédo moins élevé induite par l'érosion, ainsi qu'aux changements sur la température et l'humidité relative de la couche limite.

TABLE OF CONTENTS

LIST OF ABBREVIATIONS

a.s.l.: above sea level

AP: Antarctic Peninsula

AST: Aeolian snow transport

BSM: Blowing snow module

MAR: Modèle Atmosphérique Régional

s.l.r.: sea level rise

SMB: Surface mass balance

I. INTRODUCTION

In July 2017, media covered the calving of one of the biggest icebergs ever recorded. The A68 iceberg was calved from the Larsen C ice shelf. With an area of 5800 km², it represented approximately twice the size of Luxembourg. Media extensively covered that event and made the link with climate change and associated ocean warming in the Weddell Sea.

This is just one of the headlines relating to climate change and its impacts on the cryosphere one can read on a weekly basis these recent years. The polar regions are the ones the most sensitive to atmospheric and oceanic warming, causing (with other factors) the Greenland ice sheet to lose mass, arctic sea ice extent to reduce every winter, and much more. Because of this extreme sensitivity, they progressively became the 'thermometer' among the media when it comes to climate change and its impacts; what happens there tends to give the rest of the world an indication on the whole global situation.

Figure 1 - A map of the Antarctic continent. Ice sheet is in white, while ice shelves are in grey. Source: Landsat Image Mosaic of Antarctica (LIMA) project.

With its pole-centered, isolated situation (Figure 1), the Antarctic continent (14,200,000 km2 i.e. approximately 25 times the size of France) seems so far less sensitive to those changes than the Arctic region. Yet, it regularly hits the newspapers' headlines, which now often underline the sensitivity of West Antarctica ice shelves to warming oceans or even the changes in atmospheric circulations.

The fact is that Antarctica represents the largest component of the global cryosphere: 85% (Church et al., 2013) of all frozen waters on the globe are stocked on the Antarctic continent. If all that ice melted, this would represent a rise in sea level of approximately 62 meters. In comparison, Greenland represents 7 meters seal level rise. This is maybe why Antarctica brings so much attention in the media.

The Antarctic continent cannot be reduced to the inner plateau, where temperature is never positive and where almost no precipitation falls on the surface. Coastal regions, relatively warmer than the rest of the continent and presenting more complex geomorphic features, are places where a lot of different physical processes take place, causing remarkable spatial variabilities. Among them, the Antarctic Peninsula (AP) is worth a look, given its northernmost location and steep topography. All the accumulation and ablation of mass processes are present and vary greatly in space. This makes the peninsula a particularly appropriated case for studying variations in climate, mass balance and the interconnections between all the competing processes. Among those, the erosion of snow by the wind is here for the first time taken in account in MAR over the AP and its role on the representation of surface mass balance (SMB) is specifically investigated through a comparative study.

This work aims to study the climate of the Antarctic Peninsula and the resulting SMB over the last 39 years. With the help of a regional climate model (MAR), we simulate the climate and SMB over that period, evaluate the performance of the model, test two different configurations and discuss the differences in the results due to the accounting of aeolian snow transport processes.

In the next chapter (Chapter II), we give the reader some information taken from literature on geography, climate and mass balance of the Antarctic Peninsula. The condensed knowledge of the climatic features of that region leads the formulation of our main working hypothesis, that are express at the end of that chapter.

Chapter III presents the data that were used in this study to evaluate the model and to perform the simulations. It also includes a short description of the method we used to control and process them. The model MAR and its most relevant features to this study are briefly described, with a special focus on the blowing snow module (BSM), being the cornerstone of all our hypothesis.

Chapter IV first summarizes the evaluation of the model on the given time period against observations, both for climate and surface mass balance. Then, results without and with the blowing snow module are presented and discussed.

Finally, chapter V consists of a brief discussion on model features and associated biases, choices and assumptions that we made to conduct this study and reasons why we made them.

II. BACKGROUND INFORMATION AND PROBLEM STATEMENT

This chapter was built to give the reader the necessary information to understand what we study, why and what approach we choose to do it. We start with a short presentation of the Antarctic Peninsula (AP), its specific location within the Antarctic continent and the ice shelves that it includes, with a word on recent changes regarding those ice shelves and their implications (1). We then give a brief description of the climate of the peninsula, its major drivers and changes over the last decades (2). The third section addresses specifically the surface mass balance (SMB) resulting from the climate in the AP; we present the different components of the surface mass balance before reviewing estimates produced with a regional climate model. We also briefly review other methods and discuss their respective biases (3). After summarizing in a condensed way this background information about the AP (4), we finally present the objectives of this study and the hypotheses that we will test (5).

1. Geographical features of the Antarctic Peninsula

1.1. The Antarctic and the Antarctic Peninsula

The Antarctic Peninsula is an archipelago of frozen islands that constitutes the Northernmost part of the Antarctic continent. It consists of a relatively thin mountainous land ridge (between 50 and 100 kilometers wide on average) extending from 75°S to 63°S along approximately 1700 kilometers (Figure 2) pointing towards South America. It lies roughly between 55°W and 80°W. The Peninsula is, with some other minor parts of East Antarctica, one of the few land portions of the Antarctic that lies outside of the Antarctic Circle. Shaped by the Antarctandes mountains, the elevation over sea level is relatively high (Figure 3), with the highest top reaching 3,239 meters (Mount Hopes). As a result, it forms an effective barrier to the westerly winds blowing at those latitudes (cf. 2.1 below).

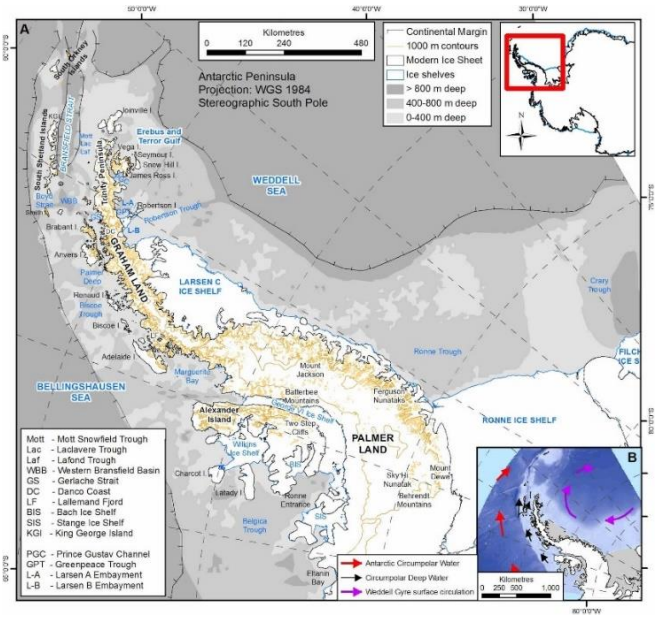

Figure 2 - General map of the Antarctic peninsula. From Davies et al. (2012)

The Antarctic Peninsula is bordered by the Bellingshausen Sea to the West ant by the Weddell Sea to the East and counts numerous small islands along the coast, the biggest one being Alexander Island to the West of the Southern half. In Weddell Sea, the Weddell gyre flows clockwise, bringing colder water from the South along the eastern coast, whereas on the West coast, the Circumpolar Deep Water brings relatively warmer water to the northernmost half of the peninsula, disfavoring the presence of persistent ice shelves there[1].

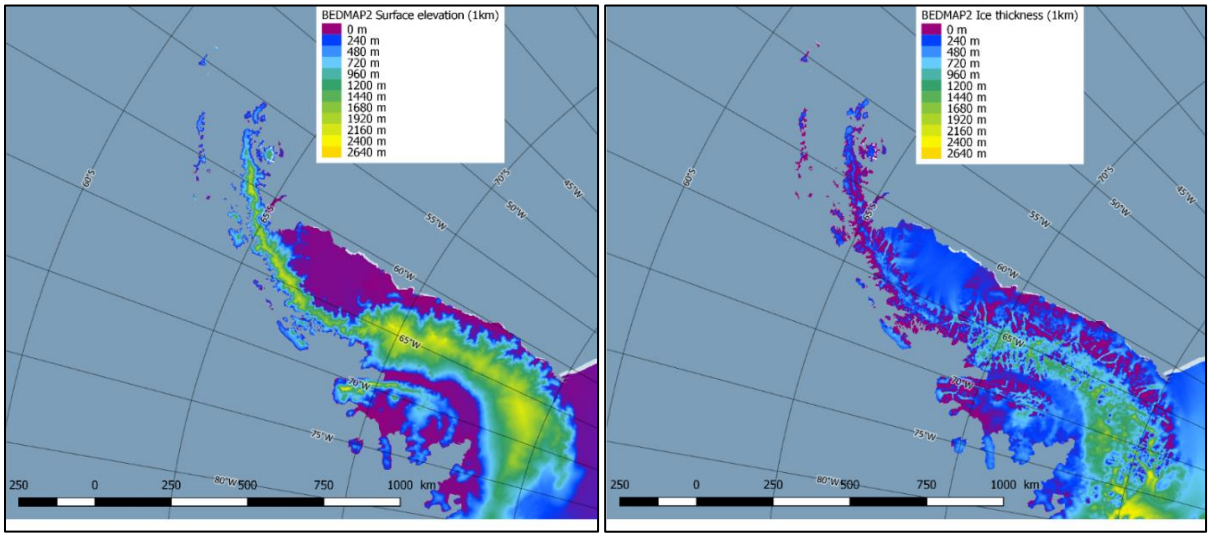

Figure 3 – Left: surface elevation (1 km resolution). Right: ice thickness (1km resolution). Data from Fretwell et al. (2013).

The thickness of ice lying on the bedrock is small compared to the rest of the continent, where it can reach 4000 meters. In the Antarctic Peninsula, it is mainly comprised between 0 and 1600 meters and it is below 500 meters for the ice shelves (Figure 3).

1.2. Ice shelves

Southeast of the Peninsula lies the Ronne Ice Shelf, which drains ice from West Antarctica. The second major ice shelf attached to the peninsula is Larsen C, one of the two last remaining components of the Larsen barrier with Larsen D, since the collapse of Larsen A in 1995 and the one of Larsen B in 2002. Larsen C has an area of about 44,000 km², i.e. roughly the area of Denmark, and like any other ice shelf, Larsen C induces a buttressing effect that slows the flow of the ice cap lying upstream, exerting a controlling effect on the contribution of the ice sheet to sea level rise in the form of iceberg discharge (e.g. Goldberg, 2017). Through this picture ice shelves must be perceived as important, active components of the ice-sheet dynamics that can be particularly responsive to climate change.

On Figure 2, the warming effect of the Circumpolar Deep Water coming to the northernmost half of the west coast is clearly visible. Since this oceanic water mass melts any formation of ice shelves from the base, no persistent ice shelf exists in that region.

[1] Ice shelves are the floating extensions of glaciers on open sea or ocean. The continuous disintegration of ice shelves at their front is referred to as calving and is the process by which icebergs are formed.

A recent study using an ice-sheet model has estimated the potential contribution to sea level rise from tributary glaciers that would result from the removal of Larsen C to 0.5 - 1.5 mm by 2100 and to 0.6 - 1.6 mm by 2300 (Schannwell et al., 2018). This is considered by the authors to be relatively low in comparison with contributions from other glaciers. However, the study of the mechanisms leading to the collapse of smaller ice shelves in the peninsula is of great interest since those involves melt, which also occurs in other parts of West Antarctica, where larger glaciers with potential greater contribution to sea level rise are present.

In the case of Larsen C, it seems that both melting at the surface and from below contribute equally to the general thinning of the ice shelf (Holland et al., 2015). However, the additional stress resulting from the infiltration of meltwater from the surface into pre-existing shelf asperity networks has dramatic effects on disintegration of the ice shelf. This process, known as hydrofracturing and possibly affecting ice shelves all around the continent, is originally caused by advection of warm air towards the ice-shelf region and absorption of solar radiation by the surface inducing melt and formation of ponds and crevasses (see 2.6 below). The most impressive calving event in the Antarctic Peninsula was the one of the iceberg A-68 in July 2017, which released an iceberg with an area of 5,800 square kilometers, i.e. roughly the size of Palestine. These changes in temperature are often attributed to either atmospheric warming or changes in the Foehn wind patterns and strength (see 2.2) in that region (eg. Luckman, 2014, Hubbard et al., 2016 and Datta et al., 2019).

2. Climate over the Antarctic Peninsula

As previously mentioned, given its fringe situation, climate over the Antarctic Peninsula is milder than in the rest of the continent and allows processes like melt and runoff to occur, while they are, so far, prohibited in more inner parts of the ice sheet due to the persistence of below-freezing temperatures even during summertime. Here we describe briefly four major components of the climate in that region, starting from atmospheric circulation (2.1) with a focus on the Foehn effect (2.2), precipitation (2.3) and the southern annular mode (SAM) (2.4). The Foehn effect and the SAM both play an important role on what follows. We then describe the role of clouds and their associated radiative forcing on the surface temperature (2.5 and 2.6). We conclude this section about climate by presenting a brief climatology of surrounding sea ice and its effect on the continental temperatures (2.7).

2.1. Atmospheric circulation

On average, atmospheric circulation across the peninsula is dominated by the strong westerlies originating from the Southern Ocean. While the formation of these westerly winds is similar to the westerlies in the mid-latitudes in the Northern hemisphere, the average magnitude is considerably higher, due to the absence of land on the major part of their trajectory. The Antarctic Peninsula forms, with Patagonia, the main portions of land that lies in those strong westerlies' track.

At 700 hPa (~ 3000 m a.s.l.), the wind speed ranges *on average* between 5 and 7 m s^{-1} from the west, being more north-westerly in the south (Figure 4). There is though a clear difference between winter and summer. While the flow is weaker and more north-westerly in summer, it is much stronger and more westerly in winter (Figure 4).

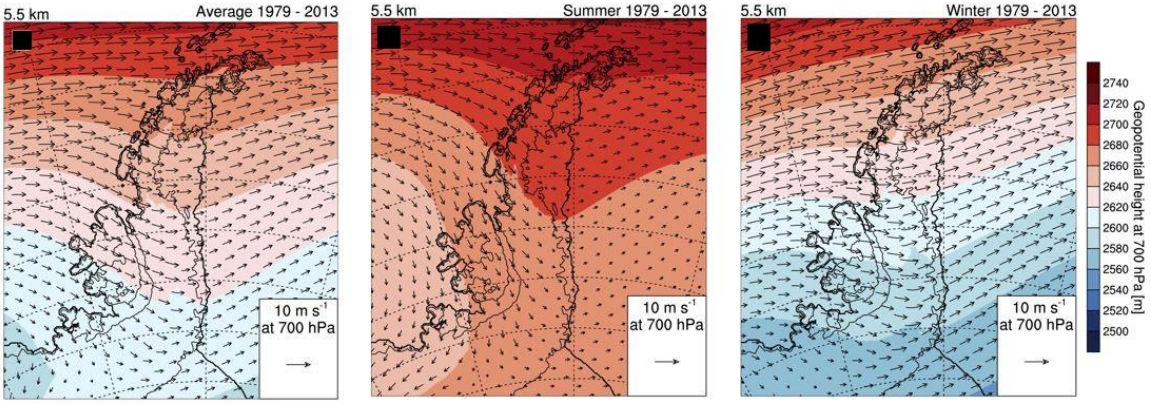

Figure 4 – Yearly (left), summery (middle) and wintry (right) averaged wind patterns (vectors) combined with 700hPa geopotential height (colors) for the period 1979-2013. Model outputs at 5.5 km resolution from RACMO2.3. Source: van Wessem et al., 2015

At 10 meters, the westerly patterns are considerably modified by the topography. The wind is on average north-westerly to northerly along the west coast and southerly along the east coast (Figure 5). As a result of the topographic barrier to the prevailing westerlies, the strongest winds occur on the western side and above the crests of the mountains. A stronger flow is also coming from the south at the southeast of the peninsula (particularly marked in winter), due to the combination of katabatic flow from the continent, ice-covered Weddell Sea and the barrier formed by the southern part of the peninsula (Parish, 1983, cited by van Wessem et al., 2015, 7314). Regarding the trends in wind patterns, if any change is significant, the magnitude is then very weak (less than +/- 0.014 m.s^{-1}).

Gonzalez et al. (2018) have built a classification of the five most frequent surface pressure patterns over the AP applying clusters on ERA-Interim reanalysis between 1979 and 2016 (Figure 6). They found that while the five most frequent patterns present similar annual frequencies, there is a large seasonal variability.

Without going into details here, what should be highlighted is that in winter, the synoptic situation with a low-pressure system over the Weddell Sea (LWS) is the most frequent (23.0% of situations in winter are classified as 'LWS'), whereas in summer the situation involving a low-pressure system over the Drake passage (LDP) is the most frequent (i.e. 28.9% of situations in summer are classified as 'LDP'). This results in relatively dry and cold air advection from south to south-west in winter and moist warm air advection in summer.

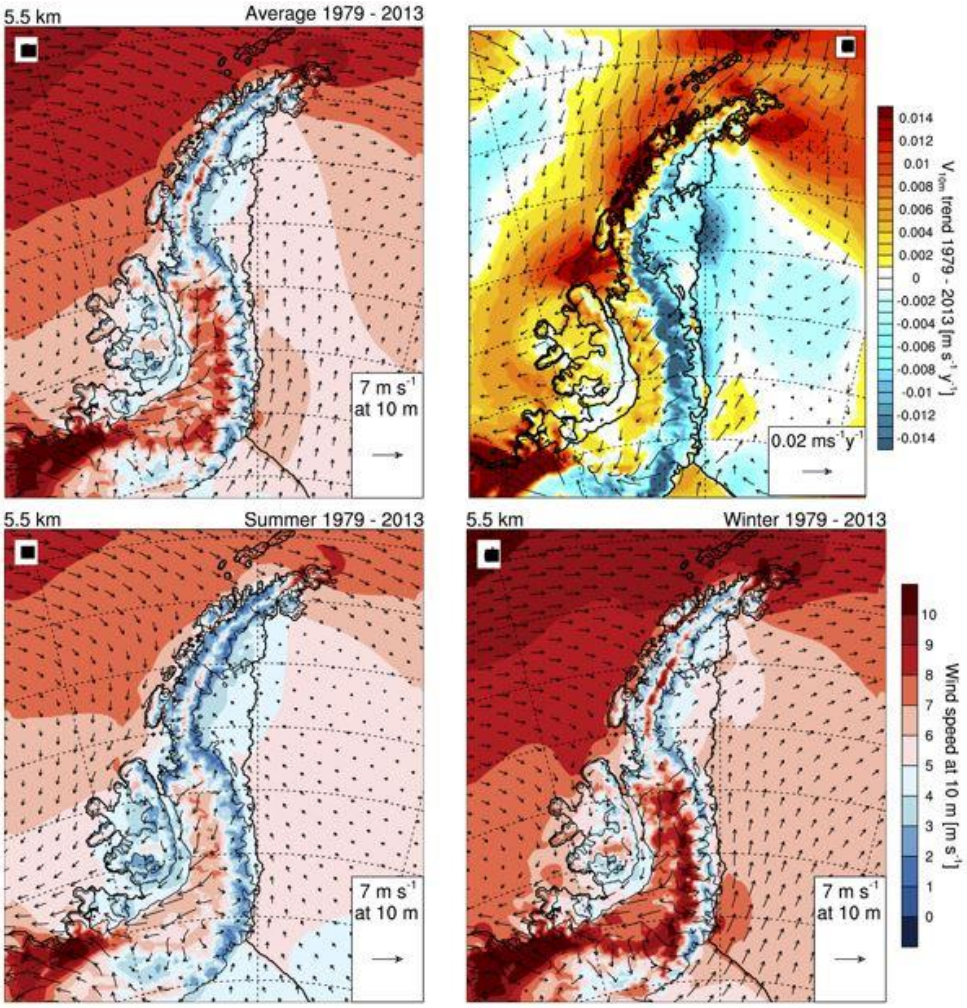

Figure 5 - Yearly (top left), summery (bottom left) and wintry (bottom right) averaged surface wind patterns for the period 1979-2013. Trends in wind patterns for the same period (top right). Model outputs from RACMO2.3. Source: van Wessem et al., 2015

The 'zonal flow over Drake Passage' pattern (Figure 6, ZDP), which is the situation favoring the most the passage of cyclones over the AP (particularly over the northern part), seems to be the a little more frequent in spring (31.5% of ZDP situations are observed in spring, against 22.3% in winter, 22.2% in autumn and 24.0% in summer[2]). Finally, the 'low over Amundsen and Bellingshausen sea' pattern (Figure 6, LAB), which consists of a low over the Amundsen and Bellingshausen Seas favoring the most the advection of warm and moist air, seems to take place mostly in spring as well (31.6% of LAB situations are observed in spring, against 23.8% in winter, 25.3% in autumn and only 19.3% in summer[2]).

[2] Calculations made on the basis of data provided by Gonzalez et al. (2018), available at: https://repositorio.aemet.es/handle/20.500.11765/7914

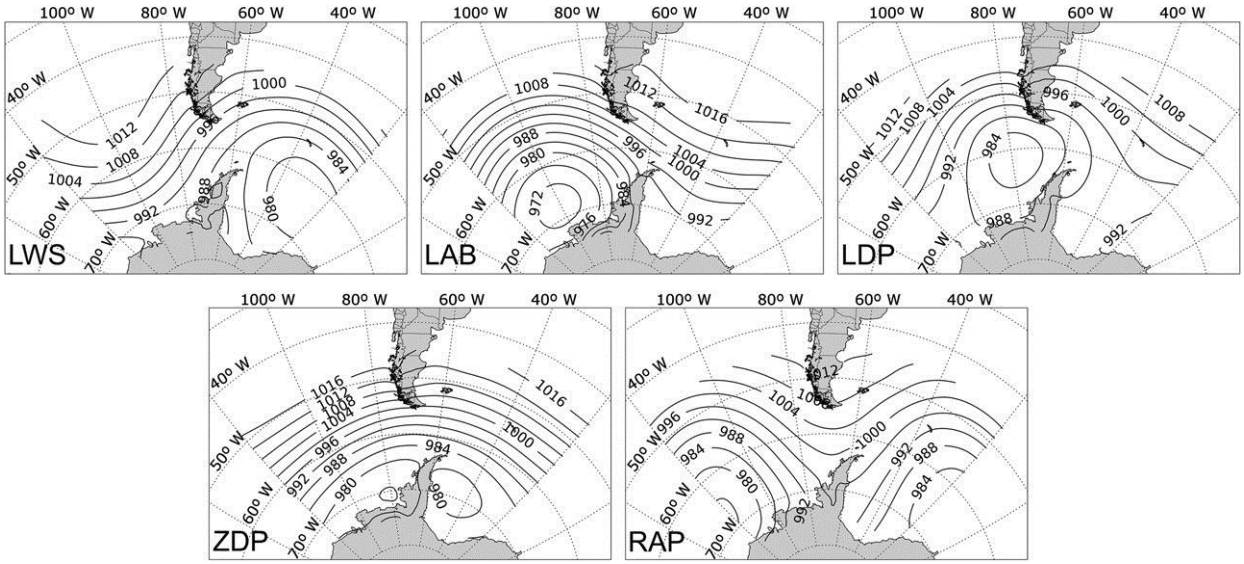

Figure 6 - Most frequent synoptic patterns calculated by Gonzalez et al., 2018. LWS: 'Low on Weddell Sea', LAB:'Low over Amundsen and Bellingshausen Sea', LDP:'Low over the Drake passage', ZDP:'Zonal Flow over the Drake passage', RAP:'Ridge over the AP'.

2.2. The Foehn effect

The Foehn effect refers to a particular wind pattern generated by the uplift of an air mass pushed towards a relief. Since the air mass is forced to rise against the topographic barrier, it cools down and condensation occurs, producing precipitation on the wind side. On the lee side, since the air has condensed out and gained heat by this process as well as through adiabatic compression, the descending air mass is drier and warmer[3].

The Antarctic Peninsula, with its high tops (cf. 1.1) situated on the track of major westerly winds in the southern hemisphere, is a major place of Foehn winds formation. Since the westerlies seem to intensify these last decades due to the positive trend in the SAM index (cf. 2.4), Foehn winds in this region are also reinforced (Turner et al., 2014 ; Marshall et al., 2006). This leads to more precipitation on the west side and warmer temperatures on the lee side, favoring melt conditions on the ice shelves that lies there (Datta et al., 2019; Luckman, 2014).

2.3. Precipitation

Precipitation consist of both liquid (rain) and solid (snow) precipitation. Their patterns on the Antarctic Peninsula present a large spatial variability. With the persistent westerly flow in that region, most of the precipitation is concentrated on the north-west coast of the peninsula (Figure 7). There is a clear gradient between the west and the east of the mountain barrier, that is explained by the Foehn effect. While the Larsen C ice shelf only receives 300 to 500 mm.yr^{-1}, the northwestern end of the peninsula receives more than 4000 mm.yr^{-1}, that is ten times more.

[3] See Elvidge & Renfrew (2015) for an in-depth study of the warming mechanisms induced by Foehn winds in the Antarctic Peninsula.

Moreover, it seems that precipitation has slightly increased in the northwest during the last decades (Figure 7). This correlates with the findings of Gonzalez et al. (2018) who identified a significant positive trend in the occurrence of LAB pattern (cf. above), denoting an enhancement of the Amundsens-Bellingshausen Seas low, which brings precipitation from the northwest. This trend has been linked to a change in the mean Southern Annular mode (see 2.4 below) phase in recent decades (Lefebvre et al. 2004). It should also be noted that a warmer climate often means more precipitation due to enhanced evaporation (Krinner et al., 2008).

It has been shown that the statistic approach in studying connections with atmospheric circulation patterns give good results and help to better understand what shapes precipitation regimes. As such, addressing those linkages in modeling studies would improve future estimates made by models only, since the latter struggle at replicating those effects (Marshall, Thompson, & Broeke, 2017).

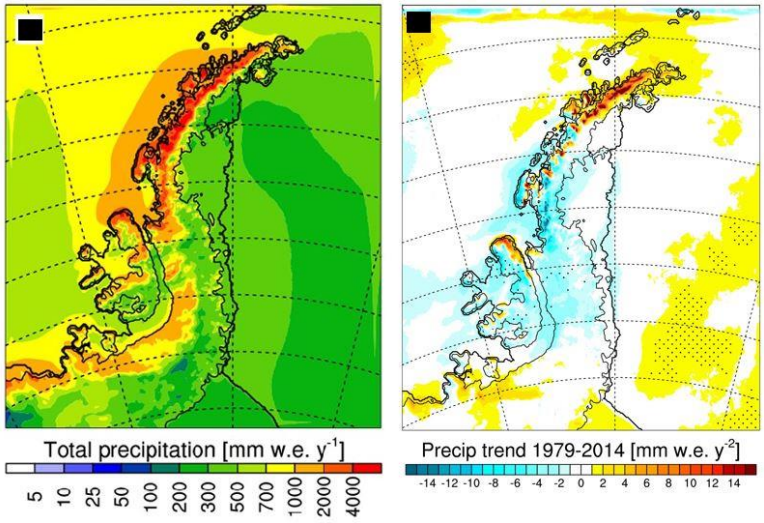

Figure 7 - Averaged precipitation (left) and precipitation trend (right) for the period 1979-2014 (dotted where significant). Regional model outputs from RACMO2.3 at 5.5 horizontal resolution, forced by ERA-Interim reanalysis. Source: van Wessem et al., 2016.

2.4. The Southern Annular Mode

The Southern Annular mode (SAM), also called 'Antarctic Oscillation', is the main mode of variability in atmospheric circulation in the high southern latitudes (Marshall, 2018). Like the *Arctic Oscillation*, it translates the 'health' of the southern polar vortex, that is the strength of the jet stream blowing above the southern polar front. The SAM index measures the difference in surface pressure between 40°S and 65°S. A positive SAM index indicates a poleward contraction of the jet belt and stronger-than-average westerlies over the mid-high latitudes (Marshall, 2018). While a positive phase of the SAM isolates the continent and thus induces cooling over most of the Antarctic, it also increases the strength of westerlies that blows across the peninsula, bringing warmer maritime air. As a result, positive SAM phases are associated

with warmer temperatures in the AP -particularly in the summer- (see e.g. van Lipzig et al., 2008), more precipitation (see e.g. Broeke & Lipzig, 2004) and enhanced Foehn winds.

Several studies have shown that the SAM index has been in a positive trend since the late 1970s, especially in summer and autumn (eg. Marshall et al., 2006 and more recently Swart et al., 2015). There does not seem to be any large consensus on the exact causes of this trend; while some authors have attributed this to the depletion of the ozone layer in the Antarctic (eg. Thompson et al., 2011), others link it with the El-Niño Southern Oscillation (ENSO) (eg. Lim, Hendon, & Rashid, 2013). The future of this trend remains quite uncertain, since the increase of greenhouse gases seems to reinforce the polar vortex, balancing and thus possibly offsetting the opposite effect induced by the present recovery of the ozone layer (Arblaster & Meehl, 2006). It should be noted though that so far, the general trend is still in a positive phase since the late 1970s.

2.5. Clouds and radiative forcing

We saw that atmospheric dynamics have an important role on the surface temperatures in the Antarctic Peninsula. Another factor of the temperature variability is the radiative forcing, especially in polar regions where snow is present (Matus & L'Ecuyer, 2017 ; Lenaerts et al., 2017). Since snow has a high albedo and water a very low one, the melt causes considerable changes in the surface radiative budget and triggers positive feedbacks.

The radiative budget of a surface is largely influenced by the occurrence of clouds and cloud properties. Clear-sky conditions are associated with large downwelling shortwave (solar) radiations during summer. On the contrary, clouds act as filters of shortwave radiations and emitters of longwave radiations. Since the peninsula lies in relatively high latitudes, there is a clear seasonal variability in incoming shortwaves, regardless the cloud amount. From a radiative perspective only, what enhances the melt in this region in winter is thus the presence of clouds, while it is more the absence of clouds that matters in summer.

Global climate models struggle to reproduce clouds their properties in polar regions (Lenaerts et al., 2017) but it seems that regional modeling produces better results with constant improvements in cloud microphysics representation (eg. van Wessem et al., 2015 ; Datta et al., 2018).

2.6. Surface temperature and melt

The Antarctic Peninsula is the area of the continent where atmospheric warming has been the strongest and the most significant since the late 1950s (Chapman & Walsh, 2007 ; Turner et al., 2014). Rather than a direct cause of Global Warming, that increase in surface temperatures over the Antarctic Peninsula have been attributed to various interconnected processes, such as changes in SAM (Marshall et al., 2006) and ENSO (Clem & Fogt, 2013), the depletion of the ozone layer (Thompson et al., 2011) and the loss of sea ice on the western side of the peninsula (Turner et al., 2013).

While a clear warming trend is visible since the late 1950s, a study identified a cooling trend since the late 1990s in the northernmost part of the peninsula (Turner et al., 2016), highlighting the important role of interannual natural variability and the impact of sea ice on surface temperatures.

As we did for the wind and precipitation (2.1), we present below the results from van Wessem et al. (2015), simulating the temperature with the regional climate model RACMO forced by ERA-Interim reanalysis for the last decades.

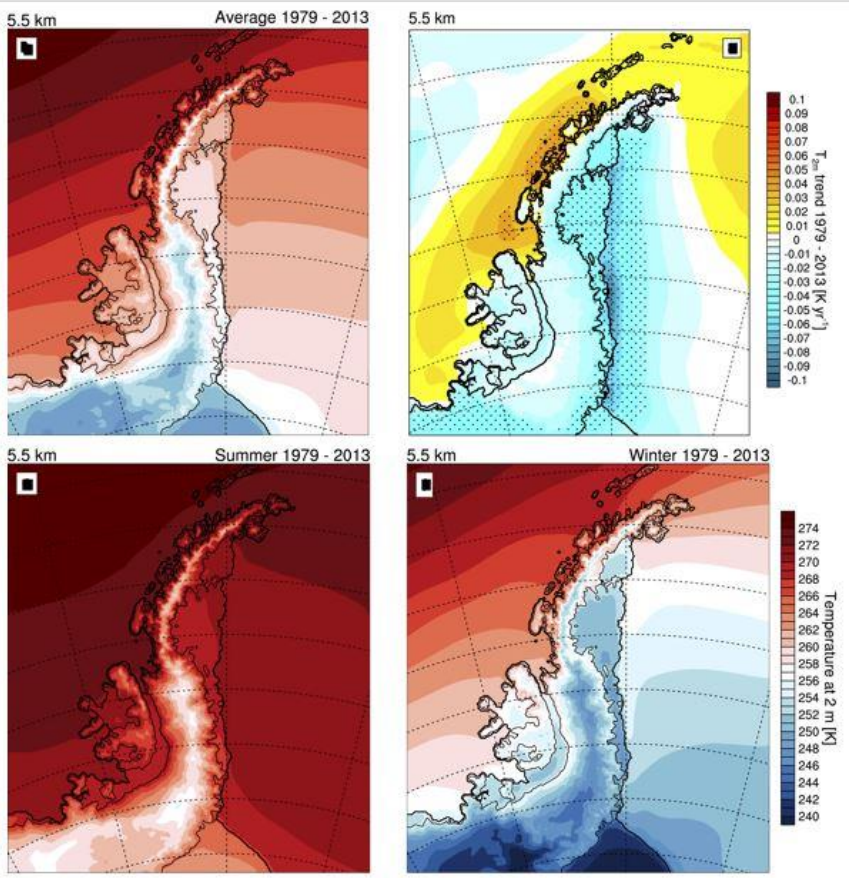

Figure 8 - Averaged annual (top left), summer (bottom left) and winter (bottom right) 2m temperature (1979-2013) simulated by RACMO2.3. Trends for this period at the top right. Source: van Wessem, J. M., et al. 2015.

The influence of topography is clearly visible, as is the cooling influence of sea ice (much more present on Weddell Sea).

While the west of the peninsula experienced significant warming (up to 0.6°C/decade), the east has conversely experiences cooling. It should be noted here that these results are annual and mask the positive trend in melt season length, occurring in summer (see eg. Barrand et al., 2013 ; Datta et al., 2018).

2.7. Sea ice

The ocean is known to provide humidity and heat to the atmosphere that is in contact with it. With atmospheric dynamics, this humidity and heat are transported towards the continents. The *continentality* of a climate is defined as the combination of climatic characteristics determined by the weakening of maritime influences towards the interior of a continent. As such, the climate in the inner parts of the Antarctica is more *continental*, while the climate on the borders and in the peninsula is more *maritime*; ocean has a greater influence over those regions. Since the heat capacity of water is much greater than the one of the air, the ocean acts like an accumulator of heat during the summer and redistributes it to the atmosphere during winter. As a result, regions with maritime climate experience a smaller seasonal variation in temperatures and receive on average more precipitation. Finally, the presence of sea ice in winter has a cooling effect on the climate, since ice cools the atmosphere above and prevents the heating of the ocean by incoming shortwaves that are to a much greater extent reflected to space because of the higher albedo of ice.

Sea-ice loss on the west coast of the peninsula has been largely documented (Turner et al., 2013 and references therein). Causes of this loss are still being investigated but it doesn't seem that recent changes in atmospheric circulation (deepening low on the Bellingshausen sea, cf. 2.1) are the main causes (id.). Rather, the origins of that sea-ice loss should be searched in ocean dynamics and heat storage (id.).

On the contrary, an increase in sea ice concentration on Weddell Sea during the last decades has also been reported (id.), leading to the cooling of the northernmost part of the peninsula, addressed by the above-mentioned study (Turner et al., 2016).

3. Observing and modeling the surface mass balance of the Antarctic Peninsula

3.1. The Surface mass balance

The (total) mass balance of an ice sheet is the difference between the total mass gain and the total mass loss of this ice sheet. It accounts for all the accumulation and ablation processes, including ice discharge (calving) and the basal melting occurring below the ice shelves.

The surface mass balance (SMB) for its part is the difference between the mass gain and the mass loss at a certain location on the *surface* of an ice sheet and for a given period of time (Figure 9). It does not account for loss by ice discharge nor basal melting. It is expressed in gigatones (Gt) or less frequently in kg m^{-2} yr^{-1}, or even in millimeter water equivalent per year (mmWE yr^{-1}) and can be calculated with:

$$SMB = P + R + S_S + ST$$

where P is the precipitation (liquid and solid), R the run-off of meltwater than has not been refrozen in the snowpack), S_S the sublimation of snow at the surface and ST the transport of snow by the wind. During transport, the eroded snow particles sublimate and can possibly be redeposited elsewhere.

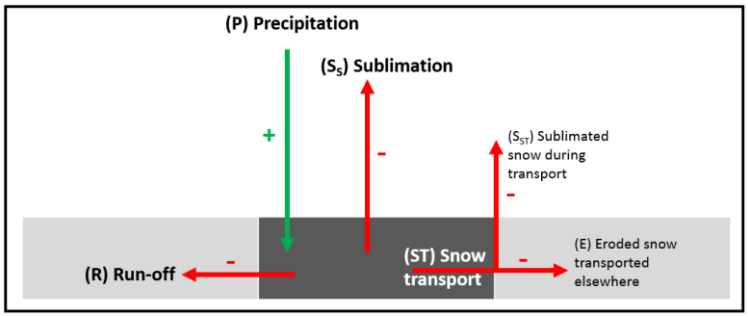

Figure 9 - Conceptual representation of SMB components for a considered grid point of an ice sheet (dark grey). Positive (negative) terms are in green (red). The two light grey cells represent adjacent grid points.

A parcel on the ice sheet can thus gain mass either by precipitation (P), condensation (i.e. negative sublimation) or by mass advected from another parcel (R or E), and loose mass from the other processes. Van Wessem et al. (2018) estimated the SMB of the Antarctic Peninsula (area 4.1 x 10^5 km²) to be on average (1979-2013) 366 Gt yr^{-1}. They found no trend in SMB values over this time span, and the integrated SMB of the peninsula has remained positive for the last three decades (Figure 10).

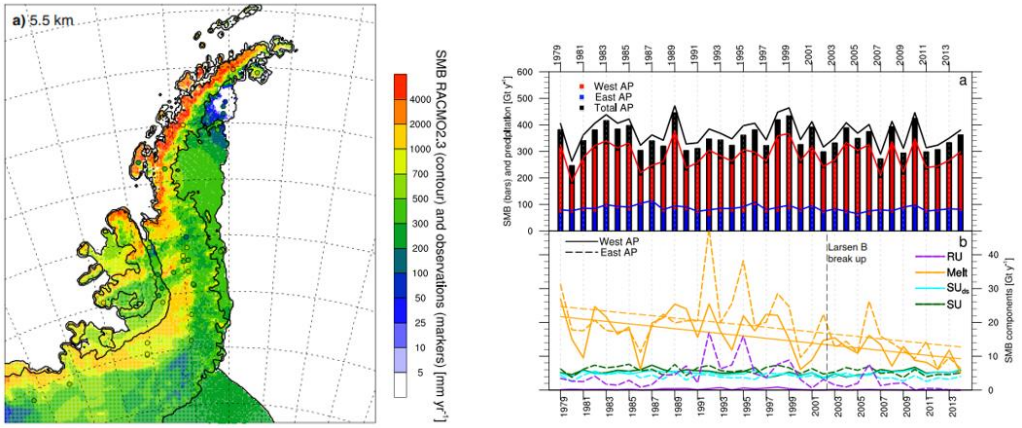

Figure 10 – Left : Averaged SMB (mm/yr) computed by RACMO2.3 for the period 1979-2013. Right : Time serie for the SMB and its components. Source: van Wessem et al. (2016).

Van Wessem et al. (2016) found large differences in the magnitude of ablation components, both between components over the whole ice cap and in quantities between the western and the eastern side (Figure 11). First, it is worth noticing that even if the Antarctic Peninsula is prone to melting, since most of melted snow refreezes in the firn, run-off is still relatively limited in magnitude, compared to other ablation terms. Indeed, it only represents 25% on average of the total ablation over the whole ice cap (and only ~ 3% in the West Antarctic Peninsula - WAP). It is however much more important (~ 42%) in the East Antarctic Peninsula (EAP), where most of the melt occurs on ice shelves.

On the windward side, aeolian snow transport[4] represents almost the totality of the ablation. On the lee side however, it only reaches ~ 40%, with even negative values for E (meaning deposition prevailing over erosion) making it an equal contributor to ablation with run-off. Finally, surface sublimation is a very small contributor to ablation in WAP and is mostly present in EAP.

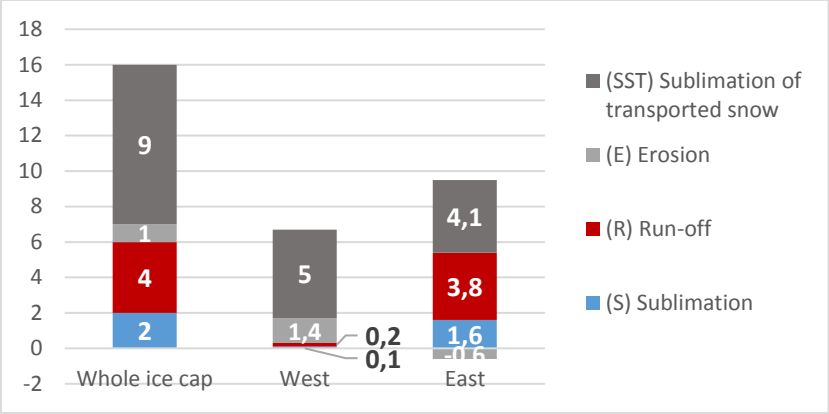

Figure 11 - Averaged figures (1979-2013) for ablation components of SMB in Gt/yr for the whole AP (left), the west PA (middle) and the east AP (right). Figures from van Wessem et al. (2016).

In the next four sections, we give some facts and figures about the four components of SMB in the Antarctic Peninsula and their spatial distribution[5].

3.1.1. Precipitation (P)

We refer the reader to section 2.1 where precipitation averages and trends have already been discussed.

We just add here that precipitation represent on average 365 Gt yr^{-1} in the total SMB, whereof 363 is snow. However, as already discussed, there is a clear west-east gradient in precipitation patterns. As such, it reaches approximately 281 Gt yr^{-1} in the west and only 84 Gt yr^{-1} in the east. Although barely significant at some places, it seems that there is a positive trend on the northwesternmost part of the peninsula.

3.1.2. Surface sublimation (S)

Surface sublimation is the sublimation of snow at a given location of the ice sheet. It must be differentiated from sublimation of transported snow, which is one of the two components of aeolian snow transport (ST). In the Antarctic Peninsula, surface sublimation accounts for ~ 2 Gt yr^{-1} and does not present any significant trend over the last decades (Figure 12).

[4] Note that the negative term in the equation is the total amount of eroded snow particles, accounting for their sublimation during transport and the redeposition of particles previously eroded.

[5] The figures in these four sections are all coming from the results of van Wessem et al. (2016) that we only cite once for all here.

There is a clear gradient visible, generally following the topographic features of the peninsula. Most of surface sublimation is observed in low areas and on ice shelves where local conditions favor the occurrence of low albedo values and an inherent increased influx of energy in the snowpack, while negative sublimation (i.e. condensation) is well visible on the crests where the saturation vapor pressure of the air is much lower due to lower temperatures.

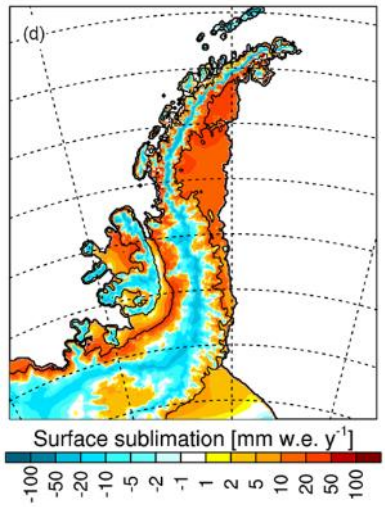

Figure 12 - Averaged (1979-2013) surface sublimation computed by RACMO2.3. Source: van Wessem et al. (2016).

3.1.3. Run-off (R)

Run-off (R) is the amount of melted snow that leaves a parcel of the ice sheet to another one, or to the sea, and that has thus not percolated nor be stored into the snowpack. It accounts for ~ 4 Gt yr^{-1} and is mainly observed on ice shelves (Figure 13). This does not mean that there is no melt, but as already mentioned above, that most of meltwater refreezes in the snowpack.

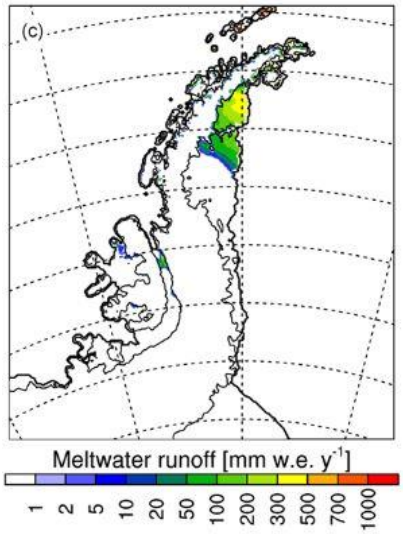

Figure 13 - Averaged (1979-2013) run-off computed by RACMO2.3. Source: van Wessem et al. (2016).

3.1.4. Aeolian snow transport (ST)

There is a large difference between the two components of aeolian snow transport. While E only accounts on average for ~ 1 Gt yr^{-1} in the peninsula, S_{ST} reaches on average 9 Gt yr^{-1}. As one could expect, erosion is mainly present on the crests and has negative values mostly elsewhere and in particular on the lee side, meaning deposition (Figure 14). Sublimation of transported snow doesn't show any clear spatial pattern, except maybe on the southeastern flanks of the mountain where it is slightly higher, mostly likely due to Foehn winds.

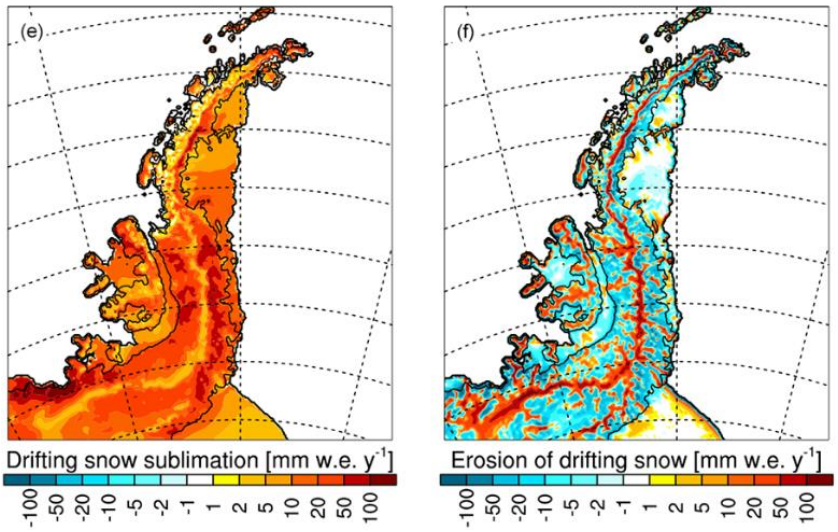

Figure 14 - Averaged (1979-2013) drifting snow sublimation (left) and erosion of drifting snow (right), computed by RACMO2.3. Source: van Wessem et al. (2016).

3.2. In-situ measurements

There are several methods to measure SMB, such as snow stratigraphy, estimates based on isotopes and radionuclides or stake measurements (see for instance Favier et al. (2013) and references therein). Among all of them, stake measurements enable for the finest temporal resolution especially for the most recent years and does not require calculation hypothesis, with additional limited measurement error (at least one order of magnitude below the actual accumulation/ablation values. For all these reasons, they are considered as the most reliable SMB measurements available for this study, and only this specific type of observations will be used for a matter of homogeneity.

Note that despite the above-mentioned advantages, stake measurements only provide a local information and does not enable the distinction between each of the SMB components.

Within the scope of the GLACIOCLIM-SAMBA project, Favier et al. (2013) recently provided an updated quality-controlled dataset for the whole Antarctic ice sheet. They stress the lack of data in highly mountainous regions (especially between 200 m and 1000 m above sea level) such as the Antarctic Peninsula. Even if their spatial coverage is very limited, those field measurements are yet necessary to evaluate models and products from remote sensing.

3.3. Remote sensing

Three main methods to estimate SMB by remote sensing can be distinguished: altimetry, gravimetry and interferometry.

Altimetry (eg. Pritchard et al., 2009) measures altitude differences over a given time span. Coupled with density estimates, this information is used to give an estimate of the SMB. Although it allows high spatial coverage, technical issues prevent this method to give good estimates on coastal regions. It is also strongly dependent on density estimates which are, just like stake measurements, very scarce.

Gravimetry (eg. Schröder et al., 2019) uses the varying distance between two satellites in row to give mass estimates. Although it gives estimates for the whole region of interest, the spatial resolution is very low and one has no information on the gravity anomaly source.

Finally, interferometry (eg. Rignot et al., 2019) uses the glaciers velocity and combine it to other information provided by regional climate models to give an estimate of the SMB over the whole ice sheet. While this method can detect mm-scale motions, it is also dependent on model results.

Although remote sensing allows more and more precise estimates to be made over the whole ice sheet, the precision remains largely under the one of direct observations, which are conversely much scarcer in space.

3.4. Regional modeling

In order to overcome the spatio-temporal coverage and resolution problems associated with in-situ measurements and remote sensing respectively, numerical modeling appears as a convenient approach. With the possibility to model surface mass balance at high resolution (the highest one being so far 5.5km – van Wessem et al., 2016), it offers a continuous, gridded SMB product that can directly be compared against observations and thus be calibrated to give an improved representation of it. Moreover, while it is impossible to measure individual components of the SMB or to retrieve it from remote sensing estimates, models allow these estimates over the totality of the studied ice sheet. It is thus, so far, the best way to have uninterrupted estimates of individual components of the SMB everywhere on the ice sheet.

To our knowledge, although the SMB of the Antarctic continent has been modeled several times with regional climate models (see Agosta et al., 2019 and references therein), the surface mass balance of the AP specifically has been the object of only two high-resolution modeling study (van Wessem et al., 2016 and van Wessem et al., 2018).

Although satisfactory, the results show that the two regional models (RACMO and MAR) used to study the Antarctic ice sheet generally accumulate too much snow on crests and not enough in valleys (Agosta et al., 2019). The authors attribute these discrepancies to possible underestimation of aeolian snow transport processes in RACMO2.3 and the absence of representation of those processes in the current version of MAR (see section 2.1 in the next

chapter discussing MAR features). These concerns are one of the main objectives of the present study where MAR will be applied at high resolution over the AP.

4. Summary

Because of its fringe geographical location within the Antarctic continent and its steep topography, the Antarctic Peninsula has several remarkable climatic features. Essentially speaking, it can be conceptualized as a wall in the middle of the ocean, perpendicular to the flow of strong prevailing westerlies. Attached to this wall, several ice shelves make up the continuity of the ice cap onto the sea and act like a buttress, slowing down the flow of the ice towards the sea.

Since the peninsula lies relatively far from the south pole and is influenced by surrounding ocean, its climate is milder than the rest of Antarctica and allows melt to occur more intensively than any other part of the ice sheet. This makes that region also more prone to warming and its glaciers more subject to decay, whatever the underlying mechanism (changes in atmospheric dynamics, sea ice loss, ozone layer depletion…). The northern Antarctic Peninsula has indeed experienced the most significant warming within the whole continent these last decades, which has caused the recent calving of some major icebergs at the front of marine-terminating glaciers and ice shelves.

With constant passage of depressions over that barrier, most of the precipitation is held on the western side. The presence of mountains also induces Foehn winds, advecting warmer and drier air on the lee side, which favors melt conditions on the eastern ice shelves and their potential destabilization. This west-east dipole pattern seems to be reinforced these last decades by the SAM index being positive more frequently, bringing westerlies poleward and enhancing their strength.

While the *total* mass balance of the Antarctic Peninsula has been decreasing the last decades with the shrink of several ice shelves, the *surface* mass balance of the Antarctic peninsula does not show any significant trend and has remained positive everywhere. Regarding individual ablation terms of SMB, aeolian snow transport is clearly the major one in the west, while it plays equally in the equation with run-off in the east, where most of the melt occurs. With scarce measurements of SMB and unprecise estimates from remote sensing, regional modeling offers considerable opportunities to have a full picture of SMB and its components over the whole ice sheet. That being said, studies on the AP SMB using regional modeling are so far very few and present several biases. Among those, authors underly the necessity to better represent aeolian snow transport processes and their influence on the representation of the climate and surface mass balance.

5. Problem statement and hypotheses

Although the most recent modeling studies on the Antarctic and the Antarctic Peninsula address the problem of aeolian snow transport in regional climate models (Agosta et al., 2019 ; van Wessem et al., 2016 ; van Wessem et al., 2018), no simulation over the AP including those processes have been performed with MAR, developed at the University of Liège, and their representation in models in that region have been poorly discussed.

Here we perform a simulation of the climate and the surface mass balance of the Antarctic Peninsula over the period 1980-2018 (38 years) with MAR (version 3.9.6). We compare outputs from simulations with and without blowing snow in order to specifically investigate the role of those processes in the model and their ability to improve (or not) the climate and SMB estimates. We evaluate the two configurations of the model against meteorological data and SMB measurements from various networks (see 'Data and methods' for details).

The main hypotheses that we test here are the following:

(1) MAR without the blowing snow module already simulates the climate and the SMB adequately. We make this assumption since this model has been specifically developed to study polar regions and has been extensively and satisfactorily evaluated over Greenland, which presents similar climatic features than the AP.

(2) **Melting rate is modified where wind-driven snow transport processes occur**. In deposition areas, since freshly deposited snow has a higher albedo than pre-existing snow, this could therefore contribute to a decrease in the energy absorbed by the surface, and therefore a decrease in the amount of energy available for the melting process. In contrast, the erosion process is likely to expose older layers of lower albedo, leading to increased absorption of solar radiations and melting.

(3) **Melting is delayed where snow is blown off the surface by the wind**. Suspended snow is more prone to sublimation (endothermic process) since it is continuously ventilated from all sides compared to surface snow. This inherent cooling of the boundary layer could possibly delay the timing of the melt season, eventually affecting the melt amount and run-off rates.

We test these hypotheses by discussing the results in chapters IV and V, after presenting the data we use to evaluate the ability of MAR3.9's to reproduce the climate and SMB of the Antarctic Peninsula and discussing some of the features of the model in chapter III below.

III. DATA AND METHODS

1. Data

1.1. Forcing data

As MAR is a regional climate model (see below), it needs to be forced at its lateral boundaries. Here we use the set of reanalyzes ERA-Interim from the European Centre for Medium-Range Weather Forecasts (ECMWF, 2009) to force MAR every 6 hours. This set of reanalyzes has been used extensively to force MAR over the Antarctic and this has overall given good results (eg.; Amory et al., 2015 ; Kittel et al., 2018 ; Agosta et al., 2019). This is also the case for RACMO, a similar model developed in Utrecht, Netherlands (eg. Wessem et al., 2018).

The variables that are prescribed at the lateral boundaries of MAR by reanalyzes are: the pressure, temperature, water vapor pressure, wind. Over ocean, sea surface temperature (SST) and sea ice concentration (SIC) are also prescribed. Every six hours, these fields, given at approximately 80 km resolution, are interpolated on the grid of MAR (here 7.5 km resolution), which then calculates its own solution beginning from the boundaries and going on inwards.

1.2. Observational data for model evaluation

We used two different datasets to evaluate the capacity of MAR to reproduce the climate and the surface mass balance of the Antarctic Peninsula: one network of automatic weather stations for the climate and networks of sparse stake measurements to evaluate the SMB.

1.2.1. Climate

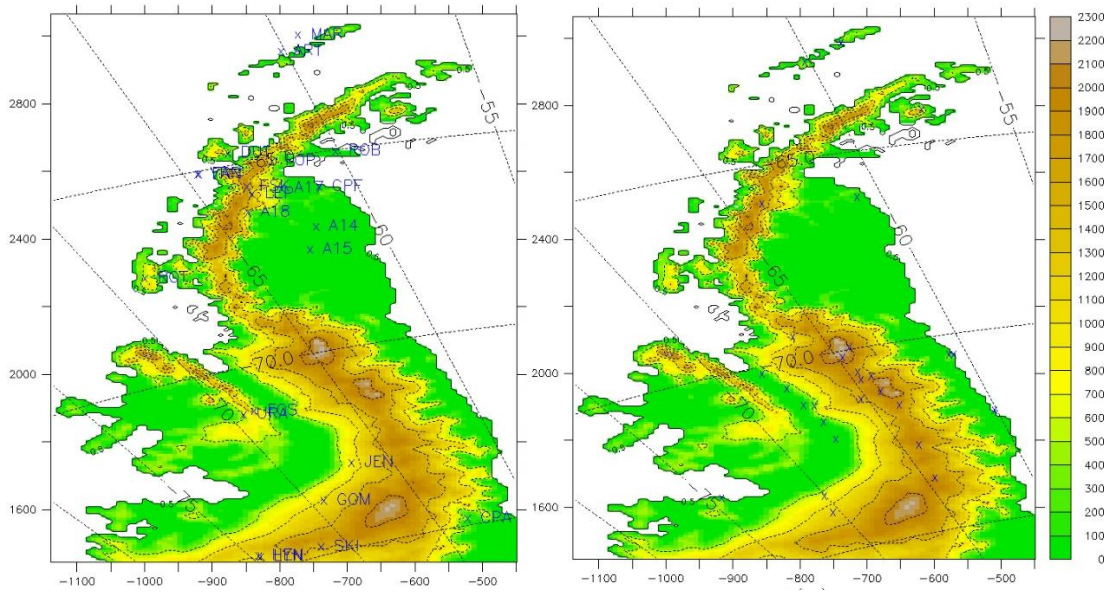

Figure 15 – (Left) Locations of weather stations used for MAR climate evaluation. Acronyms refer to station name in the table below. (Right) Location of SAMBA measurements used for MAR SMB evaluation.

Surface meteorological data (including pressure, temperature, wind, radiative fluxes and precipitation) were collected together by the British Antarctic Survey (BAS) as part of the SCAR-READER project (Turner et al., 2014) and by the Institute for Marine and Atmospheric

Research (IMAU) from Utrecht University[6]. With these two networks of stations taken together, and after the removal of unreliable stations[7] plus the ones situated in the model relaxation layer, a total of 23 stations were used for climate evaluation (see Figure 15 and Table 1). Original data were available at 3-hourly time resolution and were averaged in daily format for comparison with the model, since the outputs of MAR are daily averages.

Station name	Latitude (actual)	Longitude (actual)	Distance with center of corresponding MAR pixel (km)	Altitude of corresponding MAR pixel (m)	Real altitude (m)	Difference in altitude (m)	Temporal coverage
Cape_Adams (CPA)	-75,01	-62,53	3,61	93,08	25	68,08	1989 - 1992
Henkle_Peak (HEN)	-74,83	-73,9	4,85	1126,34	1197	-70,66	2009 - 2010
Ski_Hi (SKI)	-74,98	-70,77	1,44	1345,49	1395	-49,51	1994 -1998
Uranus_Glacier (URA)	-71,36	-68,8	3,15	715,59	753	-37,41	1986 - 2003
Bean_Peaks (BPE)	-75,95	-69,3	2,28	760,29	798	-37,71	2010 - 2012
Cape_Framnes (CPF)	-66,01	-60,55	6,69	185,21	126	59,21	2010 - 2018
Duthiers_Point (DUT)	-64,8	-62,81	6,66	177,65	78	99,65	2009 - 2014
Flask_Glacier (FSK)	-65,75	-62,88	1,1	605,28	591	14,28	2010 - 2014
Foyn_Point (FOP)	-65,24	-61,64	1,9	86,15	123	-36,85	2010 -2015
Gomez_Nunatak (GOM)	-73,88	-68,53	4,39	1357,82	1325	32,82	2010 - 2010
Jensen_Nunatak (JEN)	-73,07	-66,1	3,72	1225,94	1202	23,94	2009 -2010
Leppard_Glacier (LEP)	-65,95	-62,88	2,22	585,62	612	-26,38	2010 -2013
Lyon_Nunatak (LYN)	-74,83	-73,9	4,38	1118,34	1115	3,34	2009 -2014
Robertson_Island (ROB)	-65,24	-59,44	5,32	55,29	85	-29,71	2010 - 2018
Arturo_Prat (ART)	-62,5	-59,68	5,18	65,65	5	60,65	1983 - 2003
Faraday (FAR)	-65,25	-64,26	6,74	154,72	11	143,72	1947 - 2005
Fossil_Bluff (FOS)	-71,31	-68,28	3,85	212,8	250	-37,2	1961 - 2005
Marsh (MAR)	-62,18	-58,98	3,54	57,08	10	47,08	1970 - 2009
Rothera (ROT)	-67,57	-68,12	3,94	78,72	32	46,72	1976 - 2018
Vernadsky (VRN)	-65,25	-64,26	6,74	154,72	11	143,72	1996 - 2018
AWS14_Larsen_C_N (A14)	-67,01	-61,5	4,44	37,28	50	-12,72	2009 - 2017
AWS15_Larsen_C_S (A15)	-67,56	-62,15	3,23	39,1	50	-10,9	2009 - 2014
AWS17_Scar_Larsen_B (A17)	-65,93	-61,85	3,35	29,22	50	-20,78	2011 - 2016

Table 1 - Details for meteorological stations used to evaluate MAR

It is important to stress here that no station lies above 1400 meters, due to the difficulty to reach those particularly remote and sharp locations. A lot of the stations lies in lower areas, either on the shelves, in valleys or plains. Larsen C is relatively well covered in comparison to smaller ice shelves in the west.

[6] See the official website of IMAU for more information and data availability : https://www.uu.nl/en/research/institute-for-marine-and-atmospheric-research-imau

[7] To decide on the reliability of a station, a first screening looked at the correlation between surface pressure of all the available stations (32) and the one simulated by the model. Since pressure is a good indicator that the model performs well and that most of the stations had excellent statistics for this variable, time series of the remaining stations that had poor correlations were examined and showed discrepancies that were too high to be attributed to something else than technical failures. A total of 7 stations were then removed. A second screening looked at the remaining stations that had worse statistics than the average. Two additional stations were subtracted from the set; the discrepancies there were due to the fact that they both lied in the relaxation layer of the model.

For the sake of accuracy in the evaluation method, we did not consider stations that had an altitude difference with the corresponding MAR grid cell greater than 150 meters. Moreover, the stations situated at more than 1.5 times the resolution away from the nearest continental pixel were omitted, in order not to compare observations with values calculated by MAR for the ocean.

Like for the evaluation of surface mass balance (see next section, 'Comparison strategy'), a weighted interpolation method was used, in order to compare observations with values from several jointed pixels instead of just one.

1.2.2. Surface mass balance

Regarding the surface mass balance, we chose the GLACIOCLIM-SAMBA database (Favier et al., 2013) for the evaluation of MAR outputs. In total, 34 different measurements were used for the comparison (Figure 15).

Most of the SMB measurements were taken in the southern half of the peninsula. Unlike the meteorological stations, a lot of the surface mass balance measurements were made in higher altitude areas, which give a better sampling based on surface height here than the one for the weather. However, very few measurements were taken on the eastern shelves.

We redirect the reader to Favier et al. (2013) for further details on measurement methods, quality control and more.

Comparison strategy

We use the method used by Agosta et al. (2019) to compare the SMB observations and MAR outputs.

For each observation, we bilinearly interpolate the values computed by MAR in the four neighbor grid cells. If several observations fall into one same grid cell, we use an average of observations weighted by the time span, ie. the observations availability in time.

This method allows more consistency both in observation and modelled values. A complete description of the comparison method can be found in the above-mentioned reference and its supplements.

2. Model description

2.1. The MAR model and the surface model SISVAT

The MAR model (Modèle Atmosphérique Régional) is a regional climate model originally dedicated to polar regions and developed by the Institute of Environmental Geosciences in Grenoble and the laboratory of climatology at the University of Liège. Here we use the version 3.9.6, forced by ERA-Interim reanalyzes. As already mentioned, the variables prescribed at the model boundaries every six hours are: the pressure, temperature, water vapor pressure, wind, sea surface temperature (SST) and sea ice concentration (SIC). This model has been extensively used to simulate the climate of Greenland (e.g. Fettweis et al, 2017), but is also used for research

in Antarctica (e.g. Amory et al., 2015), in Europe (Wyard et al., 2017), Svalbard (Lang et al., 2015) and even in Africa (Gallée et al., 2004).

MAR resolves the primitive equations of the atmosphere by conserving the mass and by using the hydrostatic approximation (Gallée & Schayes, 1994 ; Gallée, 1995). This means that the vertical scale of an atmospheric flow is considered to be negligible in comparison to its horizontal scale. This is acceptable when the vertical extent of the main circulation systems (here katabatic flow and westerlies) is much smaller than the size of the grid (here 7.5 km). Nevertheless, it should be noted that non-hydrostatic processes may be active locally but represent a moderate limitation to this approach. When working at very fine resolution (less than 5 kilometers), the hydrostatic approximation loses its validity, since the resolution becomes close to the scale of typical vertical movements. Therefore, non-hydrostatic models should not be run at resolution lower than the ones of typical vertical movements.

The vertical coordinate in MAR is the normalized pressure 'sigma' (σ). It is given by:

$$\sigma = (P-P_t)/(P_s-P_t)$$

where P is the pressure at a given level, P_t the pressure at the top of the atmosphere and P_s the pressure at the surface (Figure 16).

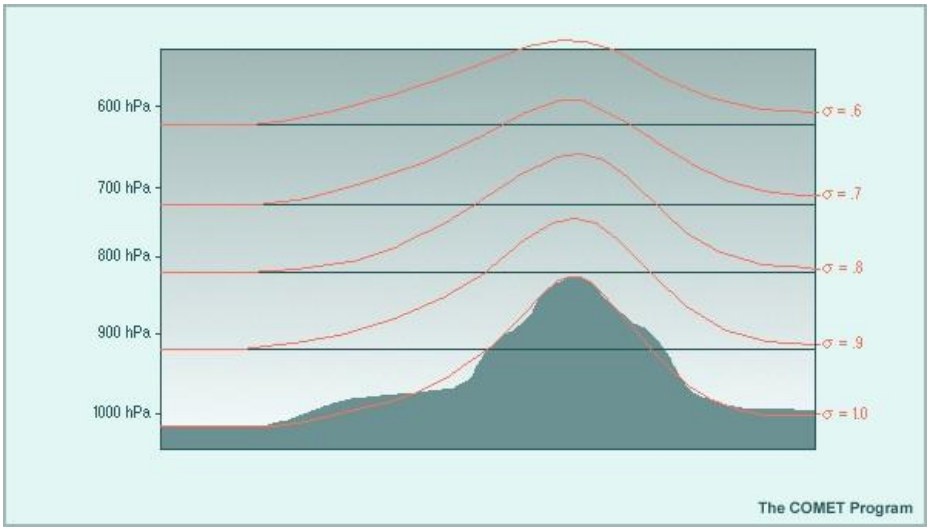

Figure 16 - Representation of sigma coordinates (Zhang, 2002)

MAR includes a cloud microphysics module that conserves the concentration in water vapour, cloud droplet, rain drop, cloud ice crystal and snow particles (Gallée, 1995). The representation of the cloud microphysical processes is adapted from Kessler (1969), with the sublimation of snow particles parametrized as a function of the relative humidity of the air according to Lin et al. (1983). The radiative scheme is the one used in ERA-40 reanalyzes (Morcrette, 2002). Vertical fluxes are calculated following the K-ε turbulence closure from Duynkerke (1988) and the representation of convection is based on the parametrization from Bechtold et al. (2001).

The atmospheric part of MAR is coupled with a one-dimension multi-layers surface model (SISVAT, Soil-Ice-Snow-Vegetation-Atmosphere-Transfer) which handles energy and mass

transfer between the surface and the atmosphere (radiative and turbulent fluxes, precipitation, erosion/deposition of snow) and the snowpack and the ground below (ground heat flux). This model includes two main modules; one for calculating heat and humidity transfers between the atmosphere and the surface (De Ridder & Gallée, 1998) and the other for calculating processes within the snow and icepacks (Gallée et al., 2001). In what follows, we use the expression 'MAR' when we refer to the MAR-SISVAT coupled model.

SISVAT includes a representation of the snowpack adapted from the one-dimensional multi-layer snowpack scheme Crocus from the CEN (Centre d'Etudes de la Neige) (Brun et al., 1992). In the present study, 30 layers are used to describe the snowpack with a fixed snowpack thickness of 20 m. An aggregation scheme automatically manages the stratification of the snowpack due to precipitation, erosion/deposition of snow, mechanical compaction, thermal and melting/refreezing metamorphism, allowing a dynamical evolution of the physical properties of the different layers over time. If precipitation or deposition occurs when the snowpack already comprises the maximum number of layers, the formation of a new layer at the surface is achieved through aggregation of internal layers. More generally, aggregation of adjacent layers is allowed according to the similarity of their physical properties. Mass and heat are conserved along the stratification process.

Note that the ice mask is fixed for the whole simulation, which does not allow changes in the representation of ice shelves extent over time. Larsen A and Larsen B are absent from the beginning (Figure 17).

The relaxation time for the model is set to 22 months, starting from the end of melt season, meaning that we start the simulation in March of year n-2 to have outputs for year n. However, we consider that outputs from year n-1 are reliable, which allow us to extend the study period from 1981 to 1980, since reanalyzes are available from 1979.

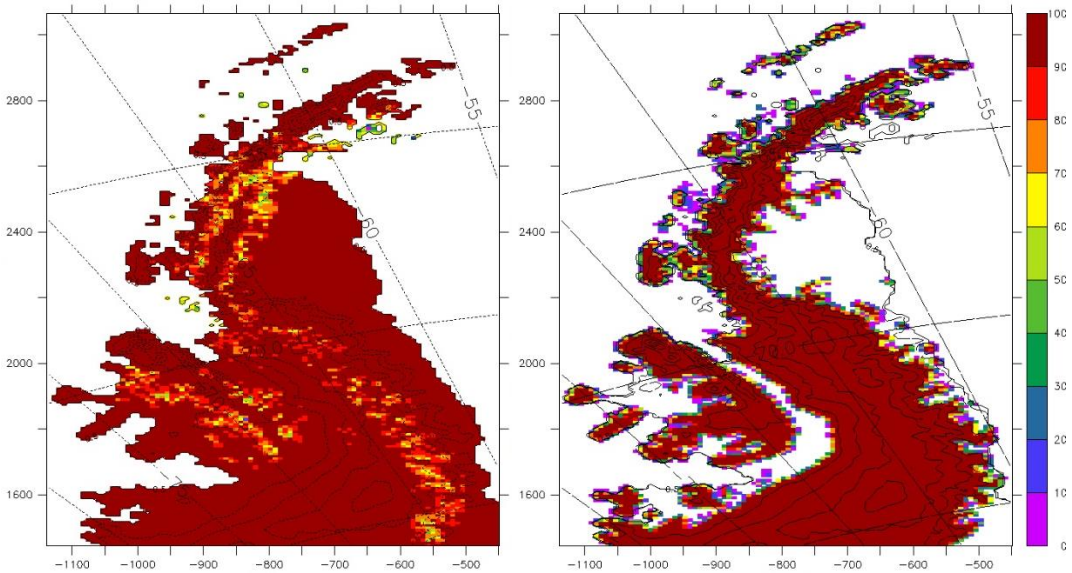

Figure 17 – (Left) Total ice mask used for the simulation, in percent of ice present by pixel. (Right) Same but for grounded ice only

The snowpack module of SISVAT contains several layers of snow or ice that interact with each other and with the atmosphere. The thermodynamic and hydrological modules are used for the calculation of heat and water transfers between the surface and the several layers. Water mass conservation allows to account for the melt, run-off, meltwater refreezing and accumulation.

The albedo is modified consequently to changes in snow/ice property (Fettweis, 2006). Those properties are determined by CROCUS, which characterizes the snow according to its temperature, its liquid water content, its density and age, as well as the size and the shape of the snowflakes (sphericity and dendricity). This allows to represent the progressive transformation of snow into firn and eventually into ice.

In practice, snow albedo progressively decreases until a minimal value of 0.65 along its densification, while it can reach a minimum of 0.4 for the ice. MAR differs from other models that do not account for meltwater refreezing and the associate change in albedo (Reijmer et al., 2012).

2.2. Blowing snow module

When the shear stress exerted by the wind on the snow surface (i.e. the friction velocity u^*) exceeds the threshold value for erosion (i.e. the threshold friction velocity u^*_t), particles become mobile and periodically bounce on the surface in a motion mechanism referred to as saltation. In even stronger winds, saltating particles are entrained from the top of the saltation layer by turbulent eddies and enter into suspension without contact with the surface.

MAR includes an erosion module (hereafter referred to as BSM) that treats aeolian snow transport (AST) processes, although they are not explicitly modeled. Initially developed to improve the representation of the surface mass balance of the Antarctic ice sheet (Gallée et al. 2001), recent modifications of the sophisticated original version have been made in order to reconcile a good representation of snow mass transport and accumulation rates (Amory et al. 2019, in preparation). In this short section, we only briefly present the module as it is now embedded in MAR; the reader can refer to the above-mentioned study for an in-depth description of the new version of the blowing snow module.

As it is the case for other processes such as thunderstorms, the transport of snow by the wind occurs at a much smaller scale that the one of MAR (here 7.5 km). Since a full representation of snow transport processes requires the use of a computationally expensive lagrangian approach to treat each snow particle and its interactions with the climate system individually, the erosion module does not explicitly model that process but rather uses a set of parametrizations that we describe hereunder.

All the AST occurs within the boundary layer of the model. Erosion at a given grid cell only occurs if u*>u*t where u*t is imposed by the uppermost snow layer properties including dendricity, sphericity and grain size (Brun, 1989), but mostly on snowpack density. This is justified by the fact that micro-properties such as dendricity, sphericity and grain size vary

greatly in space and time, leading to several hardly verifiable hypotheses. On the contrary, density estimates are more easily verifiable, and some measurements remain available for analysis. At each timestep, a quantity of snow available for saltation is computed as

$$q_{\text{salt}} = \frac{{u_*}^2 - {u_{*_t}}^2}{3.25 u_* g \rho_a h_{\text{salt}}}$$

with q_{salt} [kg kg^{-1}] the saltating particles ratio (mass of saltating snow particles per unit mass of atmosphere), g [m s^{-2}] the gravitational acceleration, ρ_a the air density. The thickness of the saltation layer h_{salt} follows the expression of Pomeroy and Male (1992): $h_{salt} = 0.08436 {u_*}^{1.27}$. The snow mass concentration is considered as constant throughout the saltation layer and serves as a lower boundary condition for the suspension layer. Snow particles are suspended through diffusion from the saltation layer just above the snow-covered surface. Suspension of snow is represented by the turbulent surface flux of snow particles

$$u_* q_{\text{s}*} = C_{\text{D}} U (q_{\text{s}} - q_{\text{salt}})$$

where $q_{\text{s}*}$ is the turbulent scale for snow particles, q_{s} and U are respectively the snow particles ratio [kg kg^{-1}] and the wind speed [m s^{-1}] in the lowest model level, and C_{D} is the drag coefficient for momentum expressed as

$$C_D = \frac{{u_*}^2}{U^2}$$

Note that if air temperature at the lowest model level is positive and/or the water content of the uppermost snow layer is not null, the blowing snow module is automatically turned off following the hypothesis that snow that has undergone melt cannot be eroded (Li and Pomeroy 1997).

Once removed from the surface, the eroded snow mass is transmitted to the atmosphere by the surface scheme. Wind-driven snow is treated by the cloud microphysical scheme as any other kind of snow particles such as snowfall, allowing for an explicit representation of the thermodynamics interactions between airborne snow particles and the atmosphere. It is however known that these two types of snow have different properties (e.g. sedimentation velocities, as explained by Bintanja 2000). Improvements on these aspects are in progress but the technical developments necessary to distinguish between snowflakes and eroded particles originating from the snow surface lie beyond the scope of this study. The uplifted snow that has gone back to the atmosphere from the ground can sublimate during transport and is advected to one of the neighbor grid cells, following the ongoing wind patterns, before eventually being redeposited to the surface according to the balance between the (horizontal and vertical) drag and sedimentation. It is consequently so far impossible to have absolute figures of erosion and precipitation when the module is turned on.

Since energy is required to maintain the uplifted snow particles in the air and these particles are subject to sublimation, the density of the air is increased, and the atmosphere is cooled down. This leads to a more stable boundary layer, which in turn inhibits the turbulence

processes. A negative retroaction involving buoyancy effects and leading to more stability is thus created when the blowing snow module is turned on. On the other hand, the increase in air density caused by the presence of suspended snow particles is responsible for an increase in the along-slope pressure gradient force and is a positive feedback in katabatic flows. A preliminary discussion of the impact of this feedback in a limited area atmospheric model is given in Gallée (1998).

2.3. Model topography

The representation of topography at 7.5 km resolution in MAR (Figure 15) has been interpolated from bedmap2 topography (Fretwell et al., 2013) available at 1 km resolution (Figure 3, chapter II). Although the extreme mountain tops (~ 2300 meters) are slightly lower than the ones in bedmap2 (~ 2500 meters), the crests are largely high enough to produce Foehn winds in MAR. This also means that the representation of topography would not be significantly improved if MAR was run at 1 km resolution instead of the one that we chose here. Moreover, at lower resolutions the hydrostatic approximation used in MAR starts to loses its validity, since vertical scales of the atmospheric flow on shorter distances become significant through acceleration due to topographic lifting (cf. above). Hence, if the model cannot reproduce them properly, it becomes less robust. A resolution of 7.5 km allows a relatively fine representation of the climate and SMB of the peninsula while ensuring not to overcome that limit.

IV. RESULTS AND MODEL EVALUATION

In this chapter, we will have a look at the model outputs on the time period 1980 – 2018. In the first section, we evaluate the capacity of MAR to reproduce the climate and the surface mass balance of the Antarctic Peninsula. We will systematically analyze the differences between the statistics for the configuration without and the one with the blowing snow module (BSM) for a range of variables and look at the spatial repartition of biases. In the second section, we will look more in details at the model outputs and the differences between the two model configurations as well. We will also have a look at the time series for some of the climatic variables, the surface mass balance and its components.

1. Evaluation of MAR

In this section, we first look at the climate of the AP (temperature, relative humidity, wind speed and radiative fluxes). For each climatic variable, we look at the spatial repartition of biases based on observations from the automatic weather stations network that we described in the previous chapter. We will also look at the integrated statistics (correlation, mean bias and RMSE) for the two model configurations.

1.1. Climate

Since regional climate models are forced at the boundaries with, among other things, pressure fields from reanalyzes, one can reasonably assume that if surface pressure is correctly modeled at a given location, the larger scale representation of pressure patterns is reliable as well. This means that surface pressure lows and highs in the regional model domain are well-positioned, which is a prerequisite for correctly modeling the climate over that region. It follows that when the correlation with pressure is high, a well simulated climate is well simulated for the proper reasons.

Here the correlation with the retained observations[8] for pressure is 0.99 both without and with the blowing snow module. Hence, this allows us to go further in the analyses of the other components of the climate over the Antarctic Peninsula.

1.1.1. Temperature

The average representation of temperature is satisfactory but seems less robust in summer (Table 2). The mean bias is increased when the blowing snow module is turned on. This is consistent with our assumptions 1,2 and 3 (cf. chapter II, section 5) that the air is cooled down by the injection of snow particles and the associated sublimation process. The RMSE is worst in winter and best in summer but does not change a lot along with the selected configuration.

[8] A first screening of the stations was carried out on the basis of correlation with pressure. Cf. 'Data and methods'.

	Correlation		Mean bias (°C)		RMSE		RMSE C	
	Without	With	Without	With	Without	With	Without	With
Year	0.93	0.94	-0.5	-1.09	2.74	2.79	2.44	2.3
Summer	0.79	0.79	-0.69	-1.08	1.64	1.88	1.28	1.36
Winter	0.87	0.9	-0.35	-1.1	3.5	3.37	3.16	2.83

Table 2 - Evaluation statistics for temperature, without and with the blowing snow module. Statistics are given for the whole year, summer only (DJF) and winter only (JJA)

MAR is too cold almost everywhere, except on the lee side of the northernmost mountain chains (Figure 18). This is possibly an overestimation of the Foehn effect by the model. Temperatures are lower systematically elsewhere where observations were available and negative biases become more negative with the blowing snow module switched on, suggesting a general underestimation of the air temperature by the model.

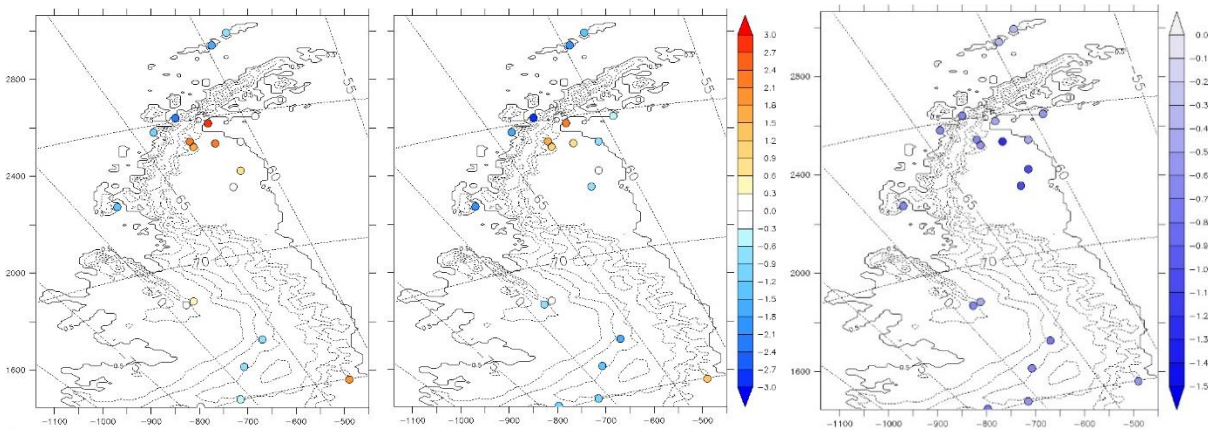

Figure 18 - MAR temperature bias for each weather station [°C]. Left: without blowing snow. Center: with blowing snow. Right: Difference between the two runs (with-without).

1.1.2. Relative humidity

MAR systematically overestimates relative humidity in the peninsula. This is obviously enhanced with the blowing snow module that moisturizes the atmosphere (Table 3) and emphasized by the underestimation of the air temperature since the relative humidity of the air is an increasing function of temperature. The error is the strongest in summer and the least in winter.

	Correlation		Mean bias (%)		RMSE		RMSE C	
	Without	With	Without	With	Without	With	Without	With
Year	0.57	0.6	6.01	6.27	9.85	9.88	6.95	6.64
Summer	0.44	0.45	7.9	8.04	10.16	10.15	6.27	6.09
Winter	0.53	0.59	4.38	4.81	9.42	9.52	6.79	6.53

Table 3 - Evaluation statistics for relative humidity, without and with the blowing snow module

The amount of weather stations measuring relative humidity and radiative fluxes being limited to only three stations all located on the Larsen C ice shelf, it is hard to tell anything on the spatial repartition of the biases (Figure 19).

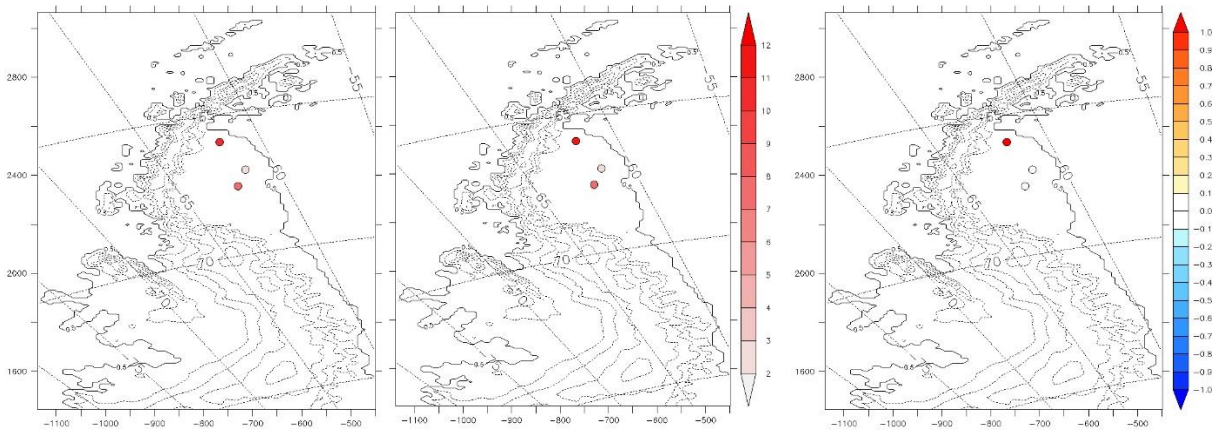

Figure 19 - MAR relative humidity bias for each weather station [%]. Left: without blowing snow. Center: with blowing snow. Right: Difference between the two runs (with-without).

1.1.3. Wind speed

Regarding the wind, averaged biases are relatively low (less than 1 m s^{-1}) and all negative (Table 4). Again here, the error is the strongest in winter. Despite the parametrization of the feedbacks between the effect of blowing snow particles on air density and the katabatic force (see III, section 2.2), the influence of the blowing snow module on the representation of wind is very weak, suggesting that these effects are not determining here, even though they enable a slight reduction of the biases. Note the slight overestimation of wind speed on the lee side of the northernmost mountain chains, consistent with the likely overestimation of the Foehn effect inferred from the analysis of temperature.

	Correlation		**Mean bias (m/s)**		**RMSE**		**RMSE C**	
	Without	With	Without	With	Without	With	Without	With
Year	0.74	0.73	-0.33	-0.27	2.61	2.63	2.36	2.4
Summer	0.7	0.7	-0.31	-0.24	2.35	2.38	2.1	2.14
Winter	0.75	0.74	-0.21	-0.18	2.78	2.79	2.52	2.56

Table 4 - Evaluation statistics for wind speed, without and with the blowing snow module

While MAR slightly underestimates the wind speed in most parts of the peninsula, it also slightly overestimates it on the eastern side of the northernmost mountain crests and on the western side of the George VI ice shelf (Figure 20).

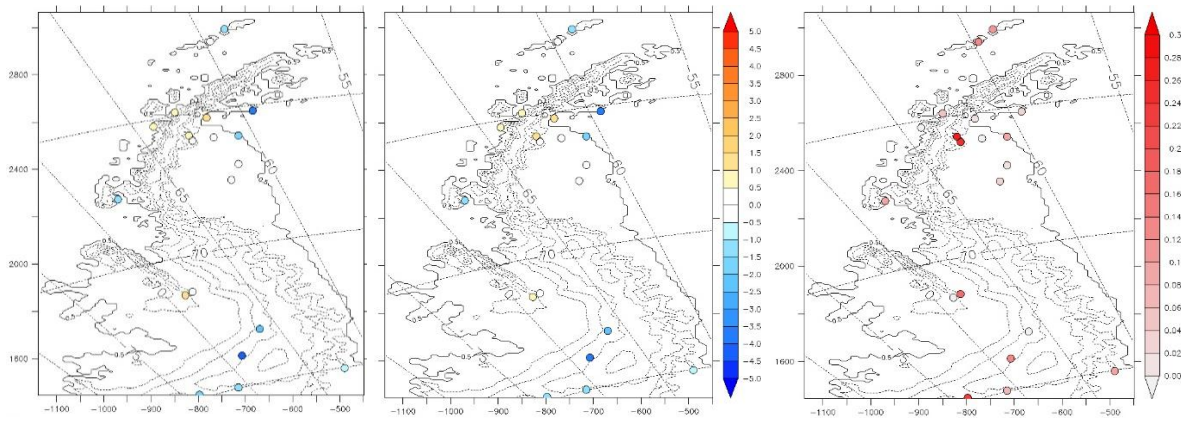

Figure 20 - MAR wind speed bias for each weather station [m/s]. Left: without blowing snow. Center: with blowing snow. Right: Difference between the two runs (with-without).

1.1.4. Radiative fluxes

Long-wave downward radiative fluxes

The representation of long waves fluxes towards the surface is particularly important for the representation of surface temperature in winter. Both the biases and the RMSE are the least in winter, but MAR still underestimates the fluxes (approximately -15W), which could also explain why the modelled average temperature is always too low. The blowing snow module has a very poor influence on the representation of the long waves downwards fluxes (Table 5).

	Correlation		**Mean bias (W/m²)**		**RMSE**		**RMSE C**	
	Without	With	Without	With	Without	With	Without	With
Year	0.75	0.75	-22.95	-21.99	33.55	32.99	24.43	24.55
Summer	0.54	0.56	-39.53	-37.17	46.18	43.84	23.8	23.2
Winter	0.73	0.75	-15.44	-14.92	25.38	25.55	20.09	20.7

Table 5 - Evaluation statistics for long waves downward fluxes, without and with the blowing snow module

Again here, it should be noted that the spatial coverage in observations is quite limited and only represents a part of the Larsen C ice shelf (Figure 21). However, this is also one of the parts of the peninsula that are the most prone to melt and consequent run-off.

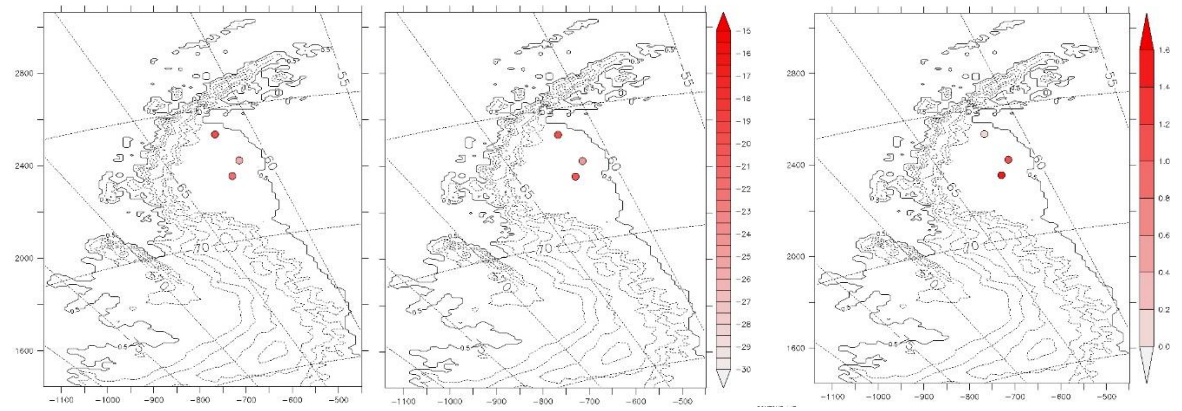

Figure 21 - MAR long waves downwards bias for each weather station [W/m²]. Left: without blowing snow. Center: with blowing snow. Right: Difference between the two runs (with-without).

Short-wave downward radiative fluxes

Here on the contrary MAR always simulates on average too much radiative fluxes from the sun (more than 20 W m² in summer, see Table 6). The blowing snow module has very little effect on the representation of those fluxes. The mean biases are ~10 W m² higher than the ones of long-wave radiation and could possibly lead to an overestimation of melt during the summer season. However, since MAR is too cold, it is not sure that those biases in radiative fluxes might significantly affect the surface conditions.

	Correlation		**Mean bias (W/m²)**		**RMSE**		**RMSE C**	
	Without	With	Without	With	Without	With	Without	With
Year	0.97	0.97	1.52	0.6	32.2	31.71	31.96	31.55
Summer	0.82	0.82	26.19	23.4	48.77	47.32	41,00	41.04

Table 6 - Evaluation statistics for short waves downward fluxes, without and with the blowing snow module

MAR only simulates less short-wave radiation at the northernmost weather station of the Larsen C ice shelf.

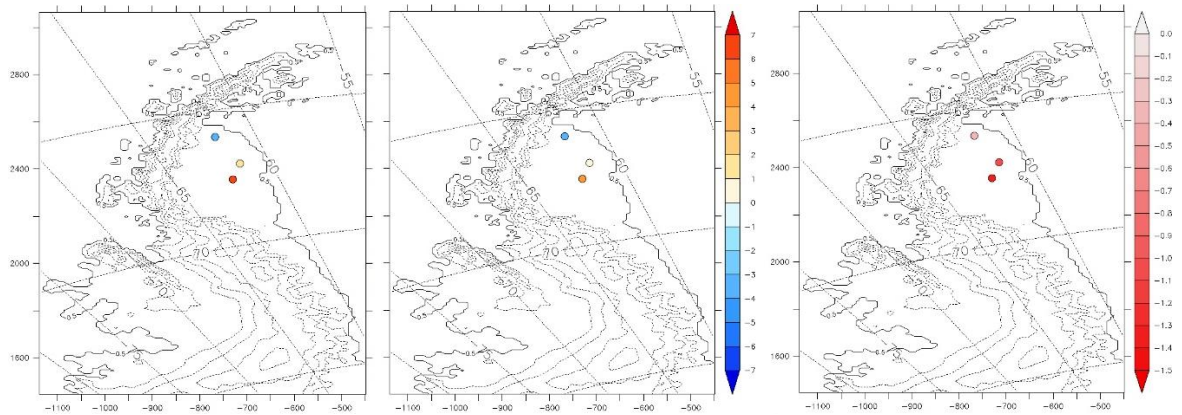

Figure 22 - MAR short waves downwards bias for each weather station [W/m²]. Center: without blowing snow. Right: with blowing snow. Right: Difference between the two runs (with-without).

1.1.5. Summary

MAR is generally slightly too cold, except on the lee side of the northern part of the peninsula, denoting a possible overestimation of Foehn winds. Enabling the blowing snow module further cools down the temperature, which is consistent with the expected cooling effect of uplifted snow particles on the surrounding atmosphere.

It seems to be also too humid, although measures of that variable, like radiative fluxes, are particularly scarce and that results should thus be considered cautiously since it might also be related to the underestimation of the air temperature. The blowing snow module further moisturizes the air, as expected.

MAR simulates the wind speed quite well, with a light underestimation and the blowing snow module has limited, although positive, effect on the representation of that variable.

Finally, the representation of radiative fluxes (downwelling short- and long-wave radiations) towards the surface presents some non-negligible biases, leading possibly to an overestimation of melt during the summer season on the eastern ice shelves. The influence of the blowing snow module on the representation of radiative fluxes is very limited.

1.2. Surface mass balance

As previously explained (Chapter II, section 3.1), surface mass balance (SMB) is the yearly averaged balance between mass gain (precipitation, deposition, condensation) and mass loss (sublimation, aeolian erosion, run-off). It can be thus considered as the resultant of the interactions between the surface climate and the upper part of the snowpack.

The model clearly overestimates the SMB where measurements have been performed (Table 7). The magnitude of this averaged overestimation approximately corresponds to 50% of the averaged observed SMB value. The RMSE is slightly higher than the observations standard deviation, meaning that the dispersion of residuals is at least equal to the observed variability. This being said, we draw attention to the fact that the standard deviation of observed values is itself very high, reflecting a strong spatial variability in the SMB of the Peninsula.

	Correlation	R^2	Average bias (m)	RMSE	Obs average (m)	Std obs
Without BS	0.81	0.65	0.27	0.46	0.55	0.41
With BS	0.80	0.64	0.22	0.42	0.55	0.41

Table 7 - Evaluation statistics for the SMB with the two configurations of MAR (without and with the blowing snow module) over the time period 1980 - 2018. Average biases and observations are given in meters water equivalent per year.

The BSM reduces the average biases up to 0.05 mWE yr^{-1}, bringing the RMSE almost to the value of standard deviation in observations. Underestimation is only observed for four of the 34 measurement sites (Figure 23 and Figure 24).

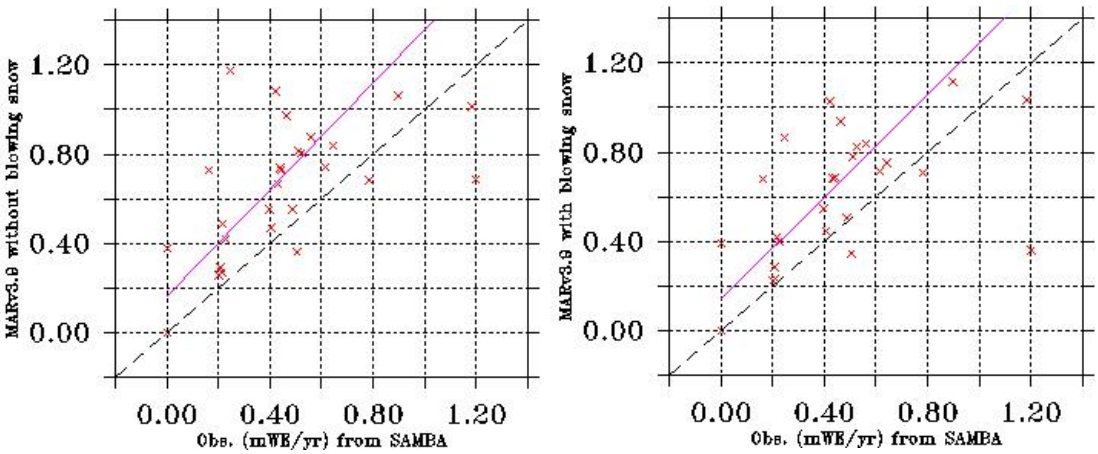

Figure 23 - Comparison between modelled and observed values for the two configurations of MAR 3.9.6: without (left) and with (right) blowing snow. Units are in mWE/yr.

The most significant improvements due to the BSM occur for the measurement sites situated on the crests (Figure 24). This is consistent with the fact that aeolian snow transport also mainly occurs in those regions, since the wind is stronger there. The underestimation of SMB seems to take place mostly in the southwest, on relatively flat areas. One exception is the strong underestimation occurring at the northernmost site (on South Orkney Islands), probably due to local geographical features badly reproduced in the model topography.

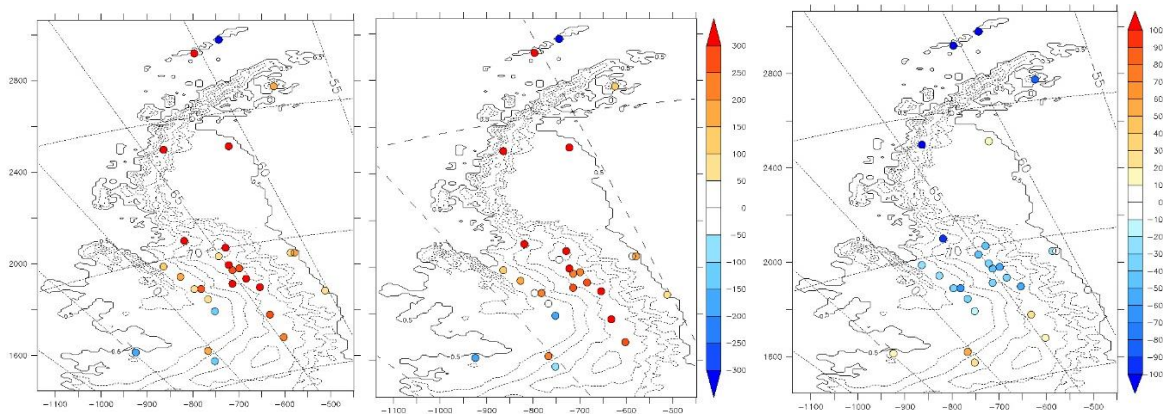

Figure 24 - Averaged biases for SMB (mm/yr) for the time period 1980 - 2018 without (left) and with (right) the blowing snow module

To conclude, we point out that, still generally overestimating the SMB, the BSM does not change any underestimation into overestimation or vice versa and it reduces the biases everywhere.

2. Results

Having now in mind how well MAR reproduces the climate and surface mass balance of the AP, here we have a look at the model outputs for the most significant variables. Climate outputs are analyzed in section 2.1 while the modeled surface mass balance and its components are reviewed in section 2.2.

For the sake of clarity, not all scales in the following figures extend from the minimum to the maximum value, but rather use infinite ends. Contours are given for surface height with steps of 500 meters (cf. Figure 15).

Since this section on results mostly looks at the differences between the two model configurations rather than the absolute values for each run, we start by looking at the outputs for aeolian snow transport as a part of the surface climate in order to better be able to discuss those differences thereafter. In section 2.2 however, AST processes are looked at as components and explanatory variables for differences in computed SMB.

2.1. Climate

2.1.1. Aeolian snow transport

As already mentioned[9], the wind-eroded snow particles not yet being differentiated from snow particles originating from clouds, it is currently impossible to distinguish each respective contribution to the suspended snow mass, prohibiting any analysis of precipitation and erosion flux separately.

However, we can calculate the total snow mass fluxes within each pixel, i.e. the total mass of snow suspended in the air and available for transport, with the following equation:

$$\Phi_s = U \times \frac{SP}{R \times T} \times Q_s$$

where Φ_s is the snow mass flux (kg/m²/s), U is the wind speed (m/s), SP is the surface pressure (Pa), R is the gas constant for air (287 J/kg/K), T is the temperature (K) and Q_s is the snowflakes concentration (kg snow / kg air). It is important to stress that Q_s is the combination of snowflakes both coming from the surface and from the clouds.

Figure 25 shows the normalized difference of that quantity between the two configurations. Overall, the BSM adds between 5 and 15% of transported snow to the run that does not account for blowing snow processes and its influence is mainly active on the lee side of the mountain chain and at the outlet of glacial valleys in the southern part of the domain.

[9] cf. Chapter III, 2.2

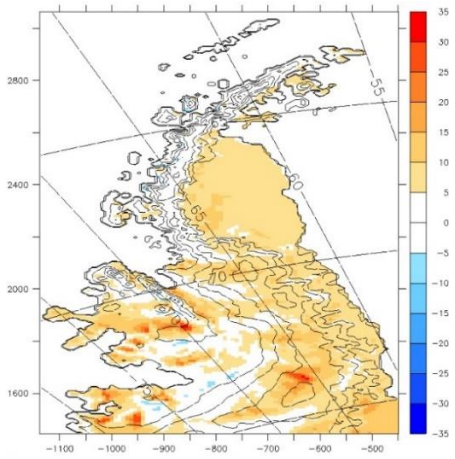

Figure 25 - Difference in transported snow mass between the two runs (with-without), normalized by the quantity of transported snow in the run with the BSM.

2.1.2. Temperature

As expected[10], when run with the BSM, MAR simulates a cooler climate than without (Figure 26). Besides increasing the temperature biases (cf. 1.1.1), this is also the first step to validate our three main hypotheses, since they are all based on this cooling effect.

The cooling induced by the BSM is significant[11], especially visible on the shelves and in winter.

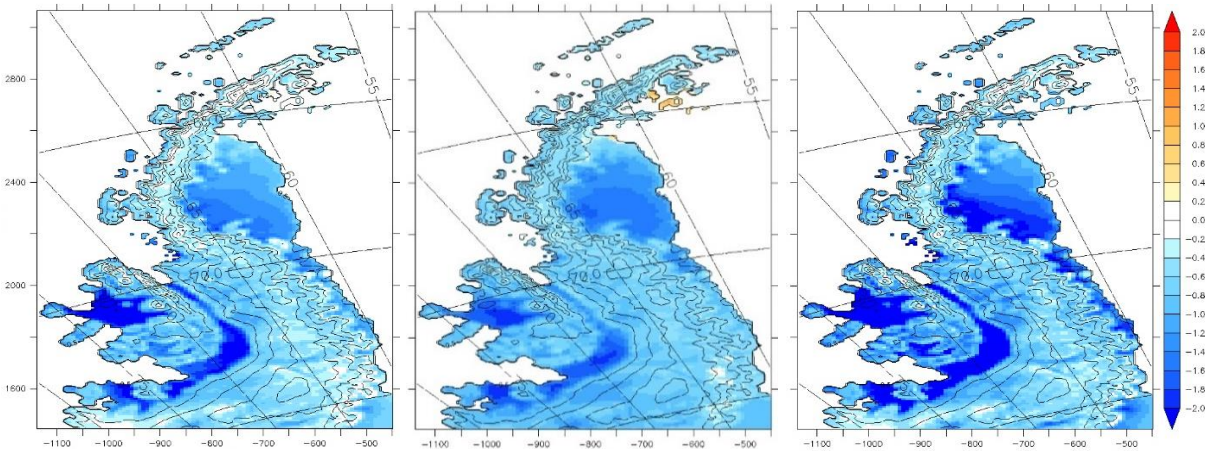

Figure 26 – Yearly (left), DJF (center) and JJA (right) differences between the two runs (with – without BSM) for temperature [°C]

Neither MAR with nor without the BSM simulate any significant trend for surface temperature throughout the considered time period over the whole domain. Discrepancies in temperature between the two model configurations remain constants, except some slightly larger differences for summer temperatures around the end of years 2000 (Figure 27).

[10] cf. chapter II, section 5: Problem statement and hypotheses

[11] i.e. higher than the natural variability.

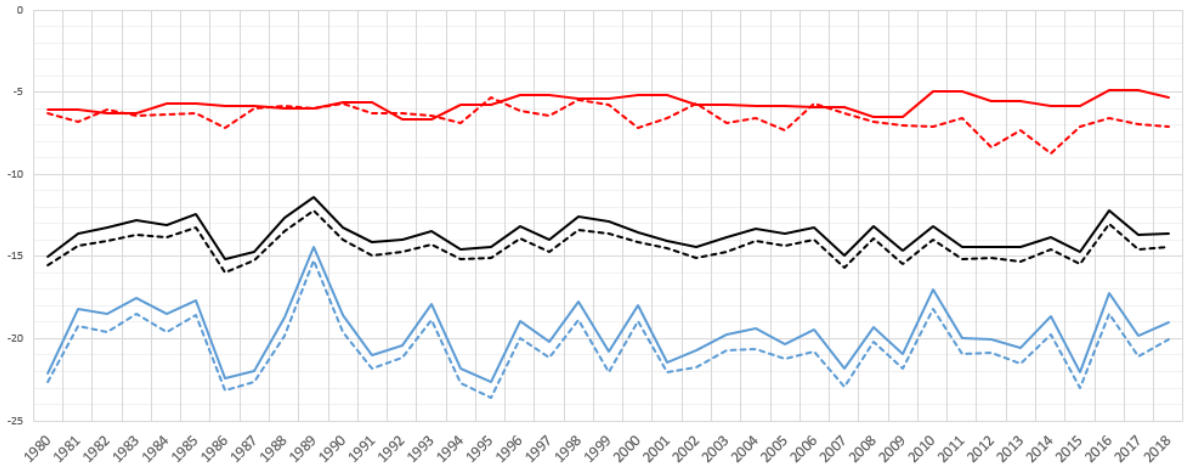

Figure 27 - Yearly (black), summery (red) and wintry (blue) temperature time series averaged for continental pixels simulated by MAR. Plain (dotted) lines are without (with) BSM respectively.

2.1.3. Wind speed

The BSM does not seem to have any significant influence on the representation of wind speed (Figure 28), supporting the conclusion that buoyancy effects of blowing snow are of minor importance in any region inside the computation domain.

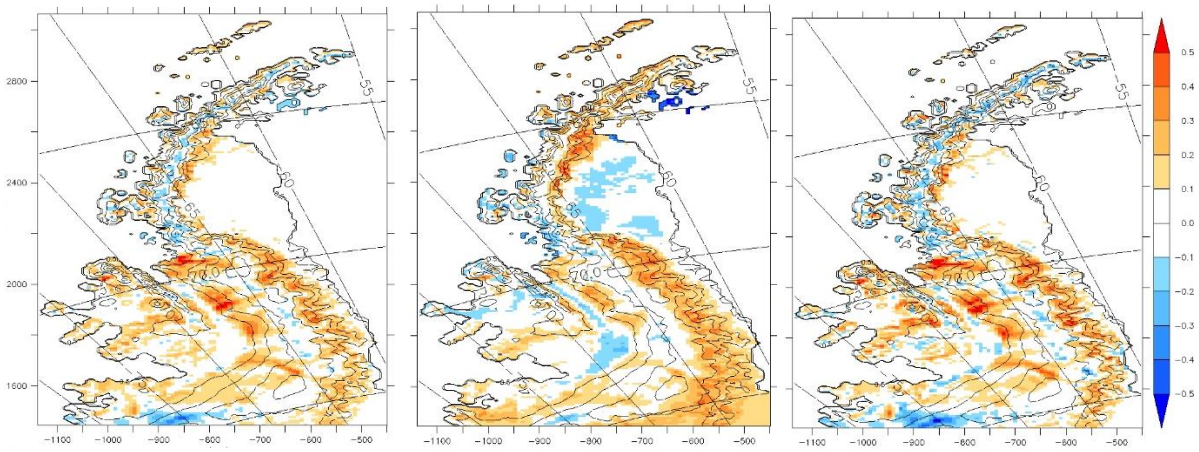

Figure 28 – Yearly (left), DJF (center) and JJA (right) differences between the two runs (with – without BSM) for wind speed [m/s]

2.1.4. Relative humidity

Differences in relative humidity induced by the blowing snow module are very weak, ranging from -2 to 2% (Figure 29). In summer, the BSM even reduces the averaged relative humidity in the north and on the eastern margins. This is most likely due to the weak differences in simulated snow mass fluxes between the two model configurations (cf. 2.1.1), suggesting that erosion rates are quite weak on average. Moreover, the BSW does not switch on when temperature is positive, which occurs very often in summer in that region.

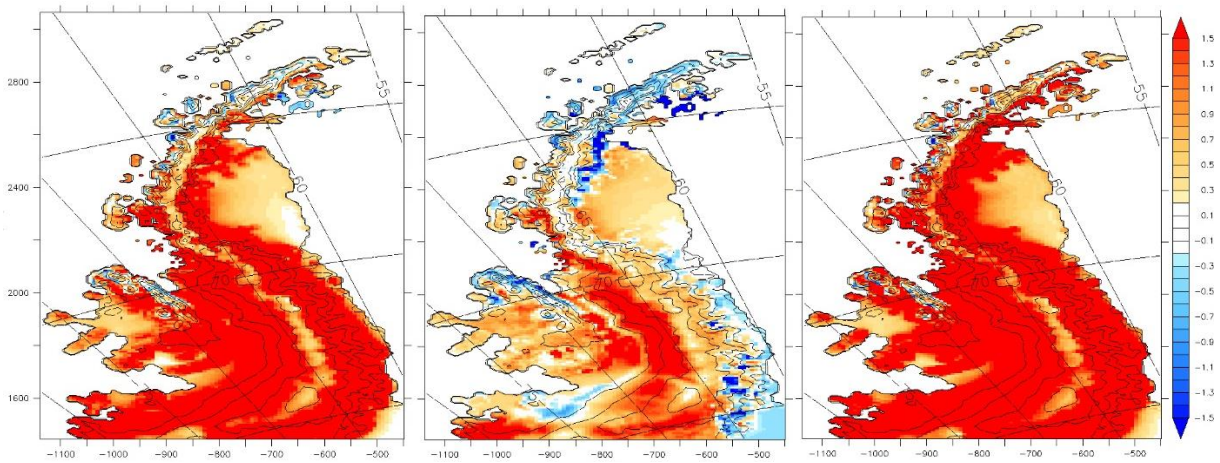

Figure 29 - Yearly (left), DJF (center) and JJA (right) differences between the two runs (with – without BSM) for relative humidity [%]

2.1.5. Radiative fluxes

Long waves downwards (LWD)

Like the wind, the BSM does not have any significant influence on the representation of long waves downwards fluxes. This suggests that the radiative contribution of suspended particles to the surface energy budget is negligible here.

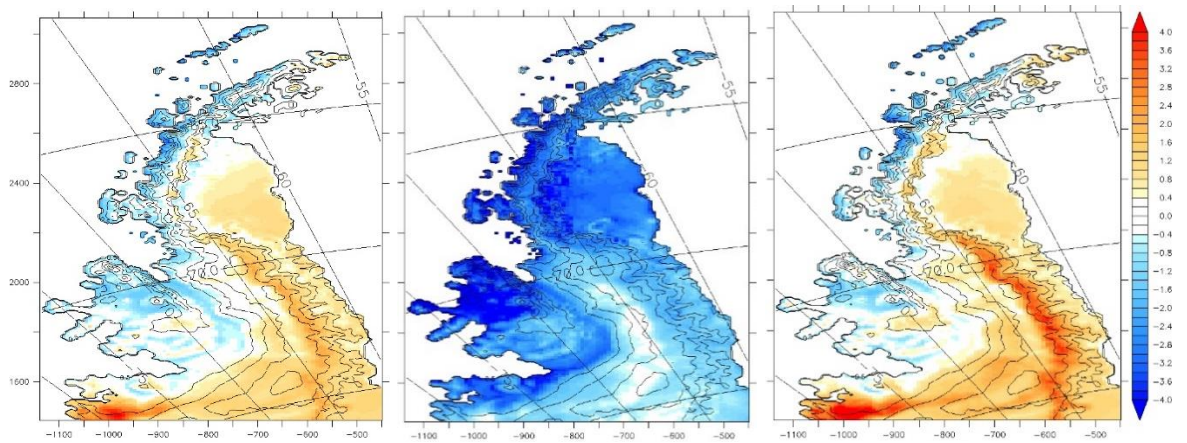

Figure 30 - Yearly (left), DJF (center) and JJA (right) differences between the two runs (with – without BSM) for long waves downwards [W/m²]

Short waves downwards (SWD)

Consistently with the effect on LWD, the BSM does not significantly impact the representation of SWD in the AP (Figure 31), although it tends to slightly increase those fluxes mostly everywhere (in summer).

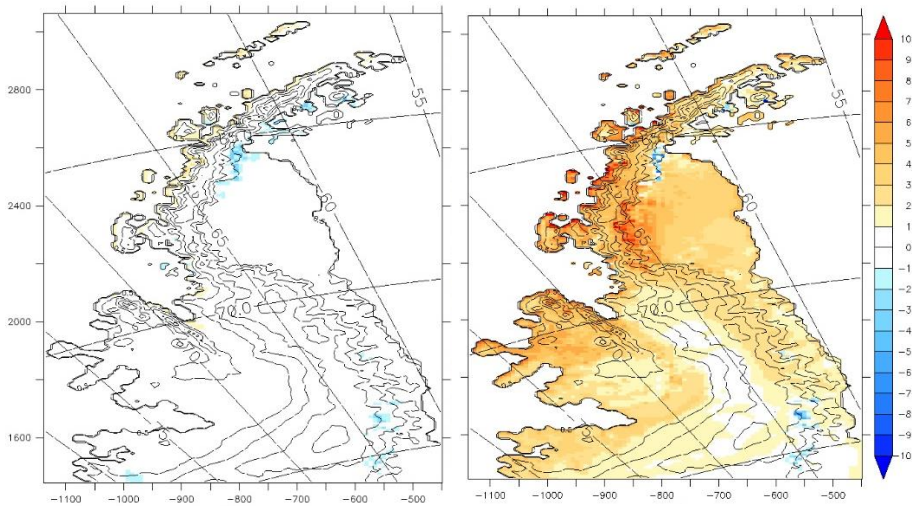

Figure 31 – Yearly (left), DJF (right) differences between the two runs (with – without BSM) for short waves downwards [W/m²]

2.2. Surface mass balance

2.2.1. Spatial variability of SMB and its components

Surface mass balance (SMB)

The averaged SMB is positive almost everywhere but presents a high spatial variability (Figure 32). The spatial gradient in the modeled SMB is strongly influenced by precipitation patterns, with the highest values being on the crests of the northernmost half of the AP. Enabling the representation of blowing snow in the model reduces the SMB almost everywhere (Figure 32), with the maximum differences being around -600 mmWE yr^{-1} in the northernmost parts of the peninsula. This suggests that blowing snow processes generally manifest as ablation processes over the whole domain. The BSM produces however slightly more positive SMB values on the windward slopes of the southern half of the AP, reflecting the effect of blowing snow deposition in the area, with maximum values reaching 160 mmWE yr^{-1}. No significant difference is observed on Larsen C ice shelf where reduced wind speed and regular surface melting inhibit the occurrence of snow transport.

It is worth noticing that despite the significant differences in temperature on the major shelves, no difference in SMB is observed in those areas. This suggests that the local effect of the BSM might produce more melt, but also more refreezing, balancing this melt overproduction.

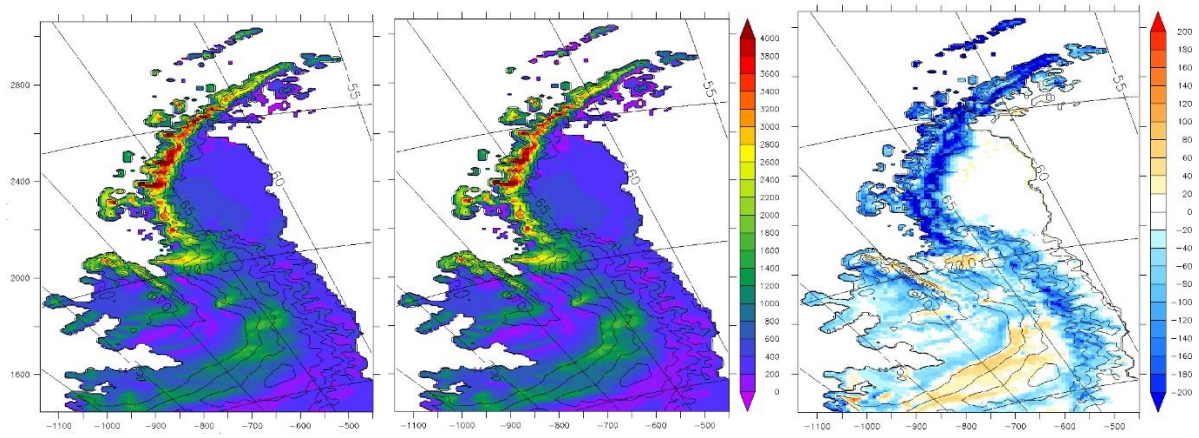

Figure 32 - Modeled SMB without (left) and with (center) BSM by MAR, averaged for the time period 1980-2018. (Right) Difference between simulation with and without BSM. All units are in [mmWE/yr]

Surface sublimation (SU)

The blowing snow module reduces the amount of sublimation mostly everywhere (Figure 33). This is in line with the cooling effect of the BSM that decreases the water vapor pressure and the increase in water vapor that reduces the humidity gradient between the surface and the surface layer, inhibiting the sublimation process.

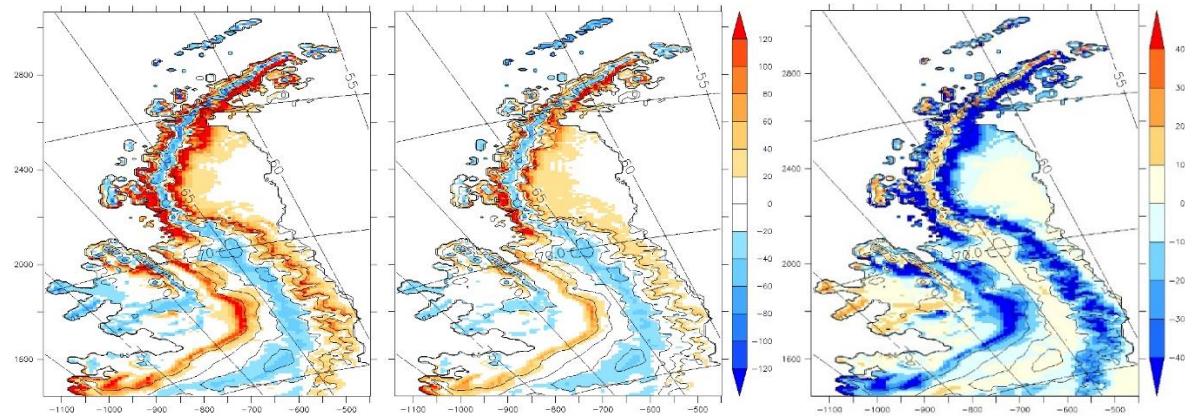

Figure 33 - Modeled surface sublimation without (left) and with (center) BSM by MAR, averaged for the time period 1980-2018. (Right) Difference between simulation with and without BSM. All units are in [mmWE/yr]

Melt (ME) and run-off (RU)

Figure 34 shows that the BSM actually enhances melt mostly everywhere in the lower parts of the peninsula, which contradicts one of our hypotheses (H1) assuming that melt would decrease in deposition areas due to higher albedo of freshly deposited snow.

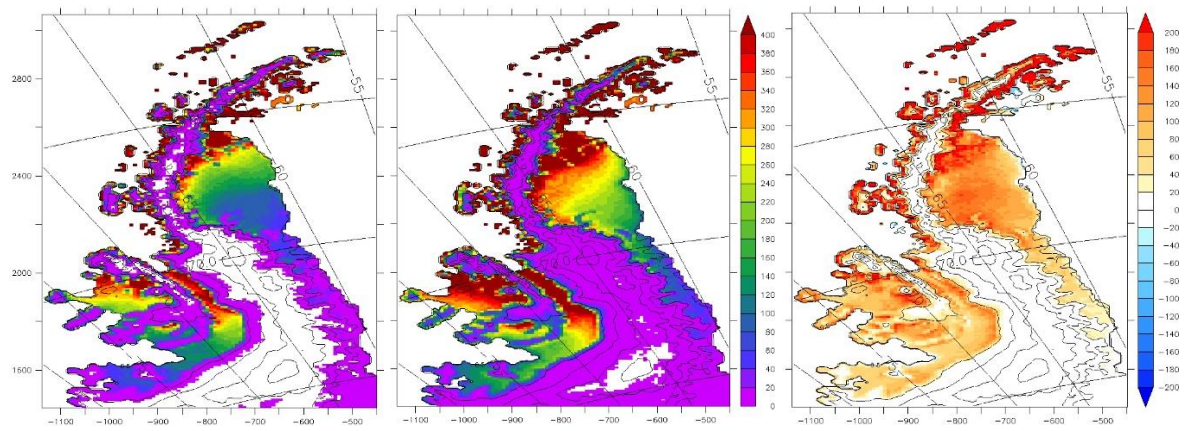

Figure 34 - Modeled melt rates without (left) and with (center) BSM by MAR, averaged for the time period 1980-2018. (Right) Difference between simulation with and without BSM. All units are in [mmWE/yr]

Run-off corresponds to the part of melted water that has not refrozen in the firn. This occurs on the shelves and in lower areas of the AP (Figure 35).

The BSM actually extends the run-off areas southwards, especially on the eastern side of the AP. It also slightly increases the amount of run-off but only in extreme north margins. We refer to the next section for more details on this amount over the whole ice sheet.

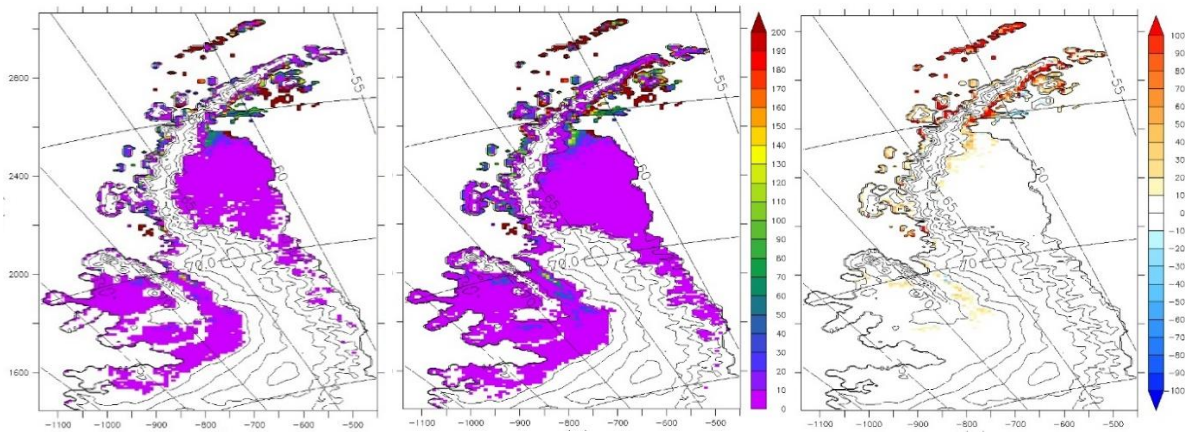

Figure 35 - Modeled run-off without (left) and with (center) BSM by MAR, averaged for the time period 1980-2018. (Right) Difference between simulation with and without BSM. All units are in [mmWE/yr]

2.2.2. Time series and average integrated SMB

Hereafter, the integrated SMB and integrated values for each of its components take in account all pixels that have more than 30% of ice (cf. Figure 17), whatever this ice is grounded or not. It thus takes in account the SMB of both grounded ice sheet and the one of ice shelves combined.

Surface mass balance

On average on the considered time period, the modeled surface mass balance of the AP varies from 300 to 450 Gt yr^{-1} (Figure 36). The SMB is reduced with the BSM by ~24.5 Gt yr^{-1}, namely a ~6% decrease.

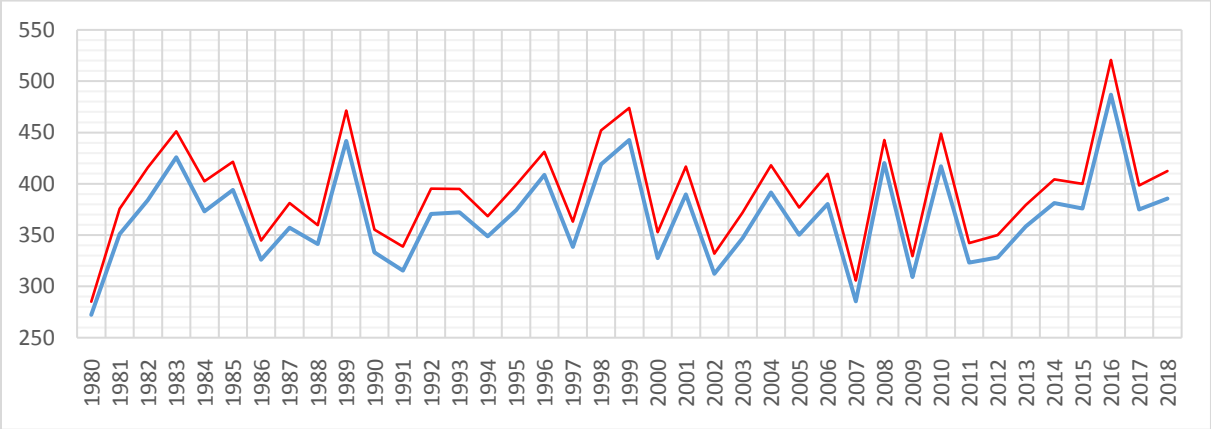

Figure 36 - Integrated SMB time series [Gt/yr] simulated by MAR without (red) and with (blue) BSM.

When the SMB of only non-grounded ice cap is considered (i.e. SMB of shelves only, cf. Figure 17), the diminution induced by the BSM is only -1.14 Gt on average, representing a ~2% decrease.

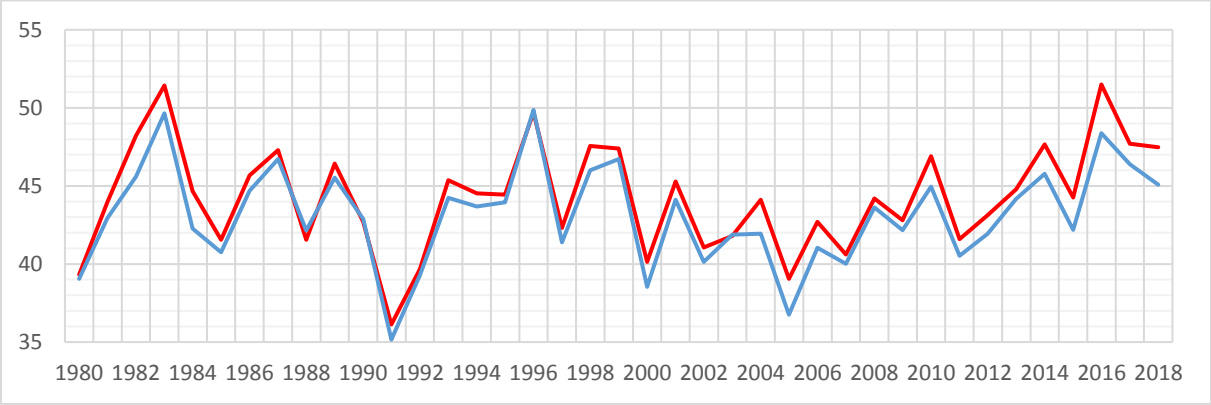

Figure 37 - Same as previous figure but for non-grounded parts of the ice-cap only.

Since an amount of snow is eroded from the surface with the BSM, it is logical to have lower SMB values when it is turned on. However, we must look at all the components together to determine how important the impact or AST on the representation of SMB is. Figure 38 presents the time series for melt, refreezing, run-off and surface sublimation.

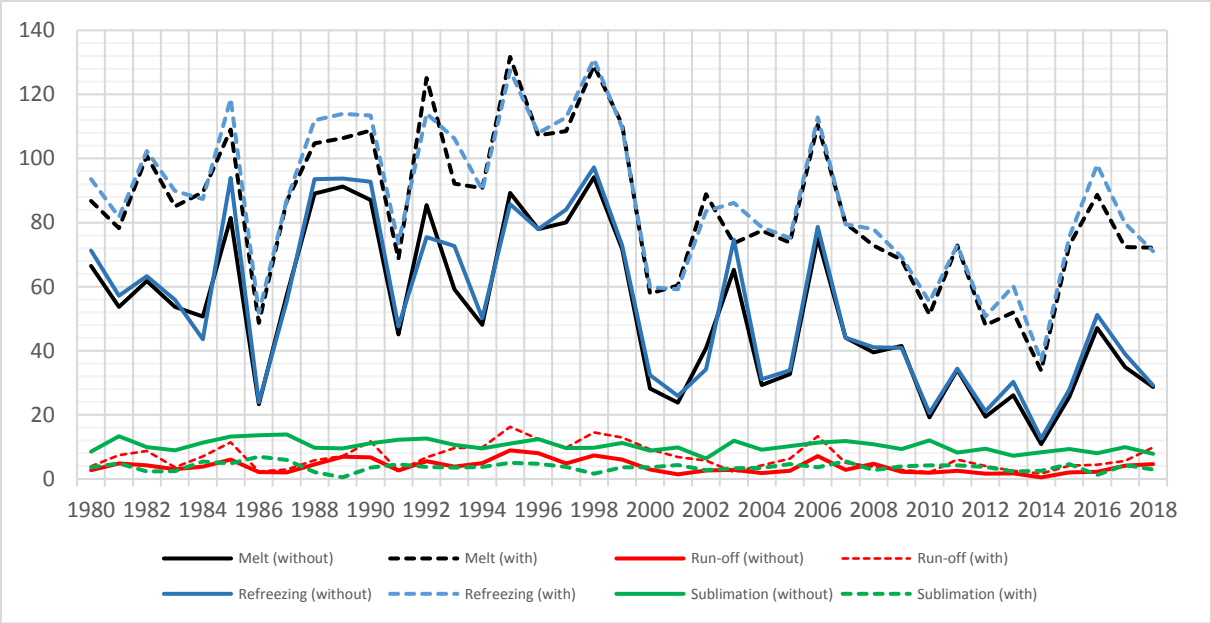

Figure 38 - Time series for melt, refreezing, run-off and surface sublimation [Gt/yr] modeled by MAR without (plain) and with (dotted) BSM

Melt, refreezing and run-off

The BSM clearly enhances processes linked to melting (Figure 39). While it cools down the atmosphere, it also enhances melt (Figure 39), which can seem counterintuitive. However, the amount of meltwater that refreezes in the firn remains more or less constant, so does the run-off.

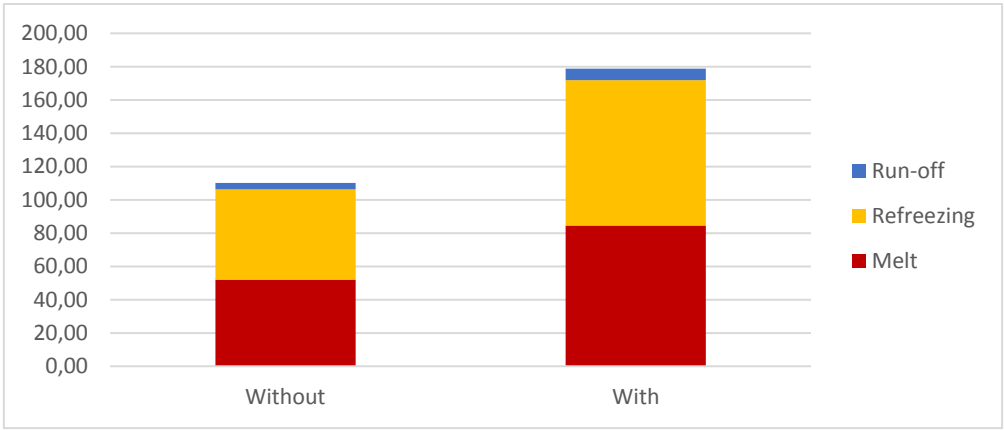

Figure 39 - Comparison between averaged values of melt, refreezing and run-off [Gt/yr] in MAR without and with BSM

One possible reason to that increase is that the albedo of freshly deposited snow on the surface is higher than the one of lower firn layers. When BSM is turned on, deeper layers with lower albedo, and thus more sensitive to radiative heating, come to the surface and receive short waves from the sun and long waves from the atmosphere. On the other hand, eroded snow from the crests that is deposited on the shelves would increase the albedo. Here this result suggests that the deposition process would not be that active and/or the quantity of snow advected toward the shelves is rather mainly sublimated on its way.

Since the eroded snow cools the ambient atmosphere, this also possibly induces more refreezing, which offset the additional melt rate and creates thus a negative feedback.

Regarding the possible delay in melt season (cf. hypothesis H3), it does not seem that the BSM induces any (Figure 40). Here we choose to look at the summer 2006-2007, when high melt rates occurred to have an idea of the temporal variability of the melt rates. While it is clearly visible that the BSM enhances melt, it does neither delay nor hasten the onset of the melt season (Figure 40). The reason to this absence of difference we see here is the same as for the enhancement of melt itself; what prevails is most likely the exposure of deeper layers with lower albedo.

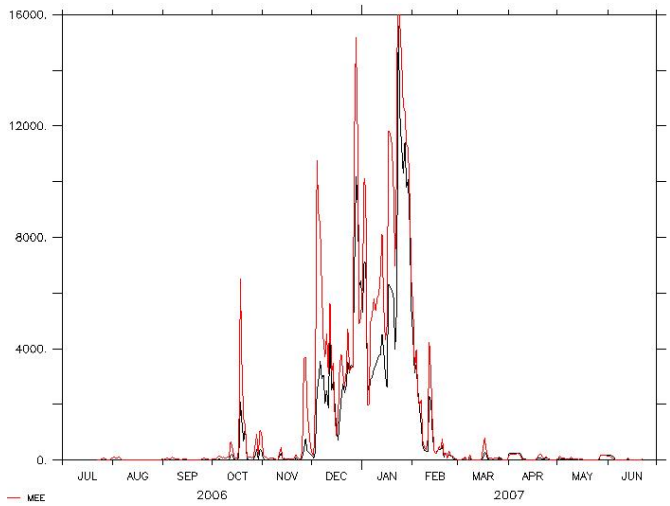

Figure 40 - Melt rates (sum of all pixels in mm water equivalent) for summer 2006-2007. Dark(red): without (with) BSM.

Surface sublimation

Surface sublimation accounts for more or less the same amount of mass loss than run-off. However, while run-off is (very slightly) increased by the BSM, surface sublimation is decreased when it is turned on (Figure 41). This is explained by a cooler atmosphere (with a decreased saturation vapor pressure) experiencing an increased water vapor pressure (due to windborne-snow sublimation) resulting in an increased relative humidity that makes it harder for surface sublimation to occur.

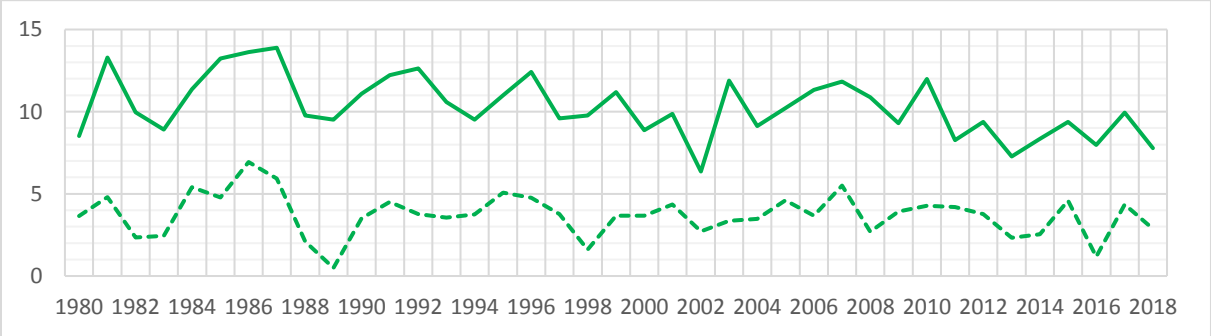

Figure 41 - Time series for modeled surface sublimation [Gt/yr] without (plain) and with (dotted) BSM

V. DISCUSSION AND CONCLUDING REMARKS

1. Hypotheses verification

Now that the results have been reviewed, we are able to go back to our main working hypothesis (II. 5) and see whether our assumptions are supported by the model outputs or not.

Concerning the ability of MAR to reproduce the climate and the surface mass balance of the Antarctic Peninsula without the blowing snow module (H1), we can reasonably say that it is the case for the climate, despite some (possible) non-negligible biases for radiative fluxes. However, the estimation of the surface mass balance presents some significant biases and should thus be taken with caution. We point out here one last time that the BSM though slightly improves the SMB statistics with a however significant reduction of the SMB (~6%) over the whole domain by acting on different components such as meltwater production, run-off, surface sublimation and most likely on precipitation but mainly through the erosion process.

We initially thought that melt would decrease in deposition areas, because of the higher albedo of freshly deposited snow (H2). Results show that the BSM actually increases both melt and run-off mostly everywhere in lower areas of the AP. The main explanation we see here is that snow might be eroded in those areas as well, at least enough to expose deeper layers with lower albedo. While melt is increased by the BSM, surface sublimation is for its part decreased, due to a cooler and moister atmosphere that reduce the water vapor gradient between the surface and the boundary layer.

Finally, MAR does not induce any delay in the onset of melt season, contrarily to what we expected (H3). Here as well, we believe that the reason is to seek in the erosion-driven exposure of deeper layers of snow with lower albedo. This process seems to prevail over the cooling of the boundary layer.

2. Methodological considerations

Given the likely important magnitude of aeolian snow transport (AST) processes in the Antarctic Peninsula (AP), their inclusion in modeling studies over that region seems now unavoidable. Here for the first time we performed simulation of climate and surface mass balance (SMB) of the Antarctic Peninsula over the last 38 years using MAR with and without a blowing snow module (BSM). The inclusion of the BSM leads to some significant changes in climate and SMB, showing that even though the AP is a warmer region where run-off regularly occurs, wind-driven erosion of snow does have a significant impact on SMB there too.

However, one limitation with the current version of MAR is that the eroded snow particles are considered as any other type of snow particles in the atmosphere. When the blowing snow module is activated, it thus becomes impossible to distinguish what comes from the clouds and what comes from the surface. Consequently, measuring the impact of the BSM on the

representation of climate and resulting SMB requires indirect calculations and preclude for now a distinct analysis of snowfall and erosion components.

Direct estimates of snow erosion are of course the first think one could look at in simulations carried out with the BSM, but the precipitation would then also be made interpretable, allowing to see for instance if the BSM induces changes in precipitation patterns. In our case, one could make (and verify) the hypothesis that the cooling of the atmosphere would lead to earlier saturation upstream the prevailing wind flows, and thus increase the precipitation there.

Moreover, to our knowledge, no measurements of aeolian snow transport have ever been carried out in the AP and reported in literature. This forced us to use a configuration of MAR that was developed for a different region (Terre Adelie), and that was also evaluated against observations carried in that region which presents very different topographic and climatic features. The climate in that flat costal region is indeed mostly controlled by katabatic winds coming from the inner plateau of Antarctica. Consequently, that region experiences much cooler and drier climate, inhibiting melt and associated processes. The properties of snow affecting the AST rates (such as density) are also different in the AP and the effects of BSM calculated by MAR rely on assumptions that are so far only verified in Terre Adelie. Ideally, a full evaluation of AST fluxes in the AP should be performed with observations made in various parts of the domain, accounting for spatial differences in wind, precipitation patterns and other relevant variables.

Among other model limitations, one could argue that the hydrostatic hypothesis in MAR makes the model less reliable in regions with steep topography where orographic uplifting is continuously taking place. Since using MAR at too high resolution might cause trouble in the model operation, due to the hydrostatic hypothesis on which it relies, the key is to find a compromise between a fine resolution and the hydrostatic model performance. But here evaluation statistics show that despite the complex topography of the AP, a hydrostatic model can still produce good results at relatively high resolution.

Given the steepness of the mountain flanks, it happens sometimes that one station used for the evaluation falls in a pixel that has a large altitude difference with the (real) one of the station, which can possibly induce a bias in temperature, for instance. To circumvent this problem, we only chose stations that had a maximum of +/-150 meters altitude difference with their associated pixel in MAR. However, unlike Van Wessem et al. (2015), we did not correct the outputs for this bias induced by altitude, because this would have prevented retroactions between variables.

Finally, another way to improve the representation of climate not by increasing the resolution (and thus by risking stability issues in the model) would have been to artificially modify values in the model topography, ie. re-sampling the digital elevation model. However, to do so would also have induced other errors (eg. if higher tops might produce more precipitation on the wind side, it might also reduce melt elsewhere).

3. Perspectives

Despite current model limitations, the representation of aeolian snow transport processes in MAR over the Antarctic Peninsula have been for the first time specifically investigated through a modeling study over the climatological period 1980-2018 (38 years) which shows encouraging results for further similar research. While the major improvements today seem to be the differentiation between the different sources of airborne snow particles, this study, carried out with a satisfactory configuration of MAR, allows other applications of MAR (with and without the BSM) over the AP.

For instance, it would have been interesting to force MAR with the new ERA-5 reanalyzes from the ECMWF and see whether they improve the model outputs in this particular region of the Antarctic or not. Future projections could also be of great interest considering the relatively high sensitivity of the AP climate within the Antarctic continent.

Given its particular relevance in that region, it would also have been interesting to evaluate the melt rates against observations from space and in-situ observations and carry out in-depth investigation on melt rates with different configurations of MAR.

Finally, we can mention here that processes actually also contributing to the SMB and especially leading to hydrofracturing and consequent icebergs calving (i.e. melt ponds formation, evaporation of liquid surface water, horizontal advection of meltwater and meltwater infiltration) are currently not taken in account in MAR. Hydrofracturing is simulated by dynamical ice caps models, but those need inputs for surface conditions from atmospheric models. Given the added value of regional models, taking such processes in account could present considerable opportunities for improving ice shelves modeling and future estimations of the contribution of ice sheets to sea level rise.

VI. REFERENCES

Agosta, C., Amory, C., Kittel, C., Orsi, A., Favier, V., Gallée, H., … Fettweis, X. (2019). Estimation of the Antarctic surface mass balance using the regional climate model MAR (1979–2015) and identification of dominant processes. The Cryosphere, 13(1), 281‑296. https://doi.org/https://doi.org/10.5194/tc-13-281-2019

Amory, C., Trouvilliez, A., Gallée, H., Favier, V., Naaim-Bouvet, F., Genthon, C., … Bellot, H. (2015). Comparison between observed and simulated aeolian snow mass fluxes in Adélie Land, East Antarctica. The Cryosphere, 9(4), 1373‑1383. https://doi.org/https://doi.org/10.5194/tc-9-1373-2015

Amory, C., Kittel, C., Agosta, C., Favier, V., and Fettweis, X. (2019, in preparation): Modelling the drifting snow climate and surface mass balance of Adelie Land, in preparation for the Cryosphere.

Arblaster, J. M., & Meehl, G. A. (2006). Contributions of External Forcings to Southern Annular Mode Trends. Journal of Climate, 19(12), 2896‑2905. https://doi.org/10.1175/JCLI3774.1

Barrand, N. E., Vaughan, D. G., Steiner, N., Tedesco, M., Munneke, P. K., Broeke, M. R. van den, & Hosking, J. S. (2013). Trends in Antarctic Peninsula surface melting conditions from observations and regional climate modeling. Journal of Geophysical Research: Earth Surface, 118(1), 315‑330. https://doi.org/10.1029/2012JF002559

Bechtold, P., Bazile, E., Guichard, F., Mascart, P., & Richard, E. (2001). A mass-flux convection scheme for regional and global models. Quarterly Journal of the Royal Meteorological Society, 127(573), 869‑886. https://doi.org/10.1002/qj.49712757309

Bintanja, R. (2000). Snowdrift suspension and atmospheric turbulence. Part I: Theoretical background and model description. Boundary-Layer Meteorology, 95(3), 343‑368. https://doi.org/10.1023/A:1002676804487

Broeke, M. R. van den, & Lipzig, N. P. M. van. (2004). Changes in Antarctic temperature, wind and precipitation in response to the Antarctic Oscillation. Annals of Glaciology, 39, 119‑126. https://doi.org/10.3189/172756404781814654

Brun, E. (1989). Investigation on Wet-Snow Metamorphism in Respect of Liquid-Water Content. Annals of Glaciology, 13, 22‑26. https://doi.org/10.3189/S0260305500007576

Brun, E., David, P., Sudul, M., & Brunot, G. (1992). A numerical model to simulate snow-cover stratigraphy for operational avalanche forecasting. Journal of Glaciology, 38(128), 13‑22. https://doi.org/10.3189/S0022143000009552

Chapman, W. L., & Walsh, J. E. (2007). A Synthesis of Antarctic Temperatures. Journal of Climate, 20(16), 4096‑4117. https://doi.org/10.1175/JCLI4236.1

Church J.A., Clark P.U., Cazenave A., Gregory J.M., Jevrejeva S., Levermann A., Merrifield M.A., Milne G.A., Nerem R.S., Nunn P.D., Payne A.J., Pfeffer W.T., Stammer D. and Unnikrishnan A.S. (2013). Sea Level Change. In Stocker T.F., Qin D., Plattner G.-K., Tignor M., Allen S.K., Boschung J., Nauels A., Xia Y., Bex V. & Midgley P.M. (eds.), Climate Change 2013: The Physical Science Basis. Contribution of Working Group I to

the Fifth Assessment Report of the Intergovernmental Panel on Climate Change. Cambridge University Press, Cambridge, United Kingdom and New York, NY, USA.

Clem, K. R., & Fogt, R. L. (2013). Varying roles of ENSO and SAM on the Antarctic Peninsula climate in austral spring. Journal of Geophysical Research: Atmospheres, 118(20), 11,481-11,492. https://doi.org/10.1002/jgrd.50860

Datta, R. T., Tedesco, M., Agosta, C., Fettweis, X., Kuipers Munneke, P., & Broeke, M. R. van den. (2018). Melting over the northeast Antarctic Peninsula (1999–2009): evaluation of a high-resolution regional climate model. The Cryosphere, 12(9), 2901–2922. https://doi.org/https://doi.org/10.5194/tc-12-2901-2018

Datta, R. T., Tedesco, M., Fettweis, X., Agosta, C., Lhermitte, S., Lenaerts, J. T. M., & Wever, N. (2019). The Effect of Foehn-Induced Surface Melt on Firn Evolution Over the Northeast Antarctic Peninsula. Geophysical Research Letters, 0(0). https://doi.org/10.1029/2018GL080845

Davies, B. J., Hambrey, M. J., Smellie, J. L., Carrivick, J. L., & Glasser, N. F. (2012). Antarctic Peninsula Ice Sheet evolution during the Cenozoic Era. Quaternary Science Reviews, 31, 30–66. https://doi.org/10.1016/j.quascirev.2011.10.012

De Ridder, K., & Gallée, H. (1998). Land Surface–Induced Regional Climate Change in Southern Israel. Journal of Applied Meteorology, 37(11), 1470–1485. https://doi.org/10.1175/1520-0450(1998)037<1470:LSIRCC>2.0.CO;2

Duynkerke, P. G. (1988). Application of the E – ϵ Turbulence Closure Model to the Neutral and Stable Atmospheric Boundary Layer. Journal of the Atmospheric Sciences, 45(5), 865–880. https://doi.org/10.1175/1520-0469(1988)045<0865:AOTTCM>2.0.CO;2

ECMWF (European Centre for Medium-Range Weather Forecasts). (2009). ERA-Interim Project, Research Data Archive at the National Center for Atmospheric Research, Computational and Information Systems Laboratory, updated monthly, https://doi.org/10.5065/D6CR5RD9.

Elvidge, A. D., & Renfrew, I. A. (2015). The Causes of Foehn Warming in the Lee of Mountains. Bulletin of the American Meteorological Society, 97(3), 455–466. https://doi.org/10.1175/BAMS-D-14-00194.1

Favier, V., Agosta, C., Parouty, S., Durand, G., Delaygue, G., Gallée, H., … Krinner, G. (2013). An updated and quality controlled surface mass balance dataset for Antarctica. The Cryosphere, 7(2), 583–597. https://doi.org/https://doi.org/10.5194/tc-7-583-2013

Fettweis, X. (2006). Reconstrution of the 1979-2005 Greenland ice sheet surface mass balance using satellite data and the regional climate model MAR. Thèse de doctorat, Louvain, Université Catholique de Louvain, inédit, 181 p.

Fettweis, X., Box, J. E., Agosta, C., Amory, C., Kittel, C., Lang, C., … Gallée, H. (2017). Reconstructions of the 1900–2015 Greenland ice sheet surface mass balance using the regional climate MAR model. The Cryosphere, 11(2), 1015–1033. https://doi.org/https://doi.org/10.5194/tc-11-1015-2017

Fretwell, P., Pritchard, H. D., Vaughan, D. G., Bamber, J. L., Barrand, N. E., Bell, R., … Zirizzotti, A. (2013). Bedmap2: improved ice bed, surface and thickness datasets for Antarctica. The Cryosphere, 7(1), 375‑393. https://doi.org/10.5194/tc-7-375-2013

Gallée, H. (1995). Simulation of the Mesocyclonic Activity in the Ross Sea, Antarctica. Monthly Weather Review, 123(7), 2051‑2069. https://doi.org/10.1175/1520-0493(1995)123<2051:SOTMAI>2.0.CO;2

Gallée, H., Guyomarc'h, G., & Brun, E. (2001). Impact Of Snow Drift On The Antarctic Ice Sheet Surface Mass Balance: Possible Sensitivity To Snow-Surface Properties. Boundary-Layer Meteorology, 99(1), 1‑19. https://doi.org/10.1023/A:1018776422809

Gallée, H., Moufouma-Okia, W., Bechtold, P., Brasseur, O., Dupays, I., Marbaix, P., … Lebel, T. (2004). A high-resolution simulation of a West African rainy season using a regional climate model. Journal of Geophysical Research: Atmospheres, 109(D5). https://doi.org/10.1029/2003JD004020

Gallée, H., & Schayes, G. (1994). Development of a Three-Dimensional Meso-γ Primitive Equation Model: Katabatic Winds Simulation in the Area of Terra Nova Bay, Antarctica. Monthly Weather Review, 122(4), 671‑685. https://doi.org/10.1175/1520-0493(1994)122<0671:DOATDM>2.0.CO;2

Goldberg, D. N. (2017). Ice Shelf Buttressing. In International Encyclopedia of Geography (p. 1‑9). Consulté à l'adresse https://onlinelibrary.wiley.com/doi/abs/10.1002/9781118786352.wbieg0567

Gonzalez, S., Vasallo, F., Recio-Blitz, C., Guijarro, J. A., & Riesco, J. (2018). Atmospheric Patterns over the Antarctic Peninsula. Journal of Climate, 31(9), 3597‑3608. https://doi.org/10.1175/JCLI-D-17-0598.1

Holland, P. R., Brisbourne, A., Corr, H. F. J., McGrath, D., Purdon, K., Paden, J., … Fleming, A. H. (2015). Oceanic and atmospheric forcing of Larsen C Ice-Shelf thinning. The Cryosphere, 9(3), 1005‑1024. https://doi.org/https://doi.org/10.5194/tc-9-1005-2015

Hubbard, B., Luckman, A., Ashmore, D. W., Bevan, S., Kulessa, B., Kuipers Munneke, P., … Rutt, I. (2016). Massive subsurface ice formed by refreezing of ice-shelf melt ponds. Nature Communications, 7, 11897. https://doi.org/10.1038/ncomms11897

Kessler, E. (1969). On the Distribution and Continuity of Water Substance in Atmospheric Circulations. In E. Kessler, On the Distribution and Continuity of Water Substance in Atmospheric Circulations (p. 1‑84). Consulté à l'adresse http://link.springer.com/10.1007/978-1-935704-36-2_1

Krinner, G., Guicherd, B., Ox, K., Genthon, C., & Magand, O. (2008). Influence of Oceanic Boundary Conditions in Simulations of Antarctic Climate and Surface Mass Balance Change during the Coming Century. Journal of Climate, 21(5), 938‑962. https://doi.org/10.1175/2007JCLI1690.1

Lang, C., Fettweis, X., & Erpicum, M. (2015). Stable climate and surface mass balance in Svalbard over 1979-2013 despite the Arctic warming. The Cryosphere, 9(1), 83‑101. https://doi.org/https://doi.org/10.5194/tc-9-83-2015

Lefebvre, W., Goosse, H., Timmermann, R., & Fichefet, T. (2004). Influence of the Southern Annular Mode on the sea ice–ocean system. Journal of Geophysical Research: Oceans, 109(C9). https://doi.org/10.1029/2004JC002403

Lenaerts, J. T. M., Van Tricht, K., Lhermitte, S., & L'Ecuyer, T. S. (2017). Polar clouds and radiation in satellite observations, reanalyses, and climate models. Geophysical Research Letters, 44(7), 3355–3364. https://doi.org/10.1002/2016GL072242

Li, L. and Pomeroy, J. W.: 1997, 'Estimates of Threshold Wind Speeds for Snow Transport Using Meteorological Data', J. Appl. Meleorol. 36, 205–213.

Lim, E.-P., Hendon, H. H., & Rashid, H. (2013). Seasonal Predictability of the Southern Annular Mode due to Its Association with ENSO. Journal of Climate, 26(20), 8037–8054. https://doi.org/10.1175/JCLI-D-13-00006.1

Lin, Y.-L., Farley, R. D., & Orville, H. D. (1983). Bulk Parameterization of the Snow Field in a Cloud Model. Journal of Climate and Applied Meteorology, 22(6), 1065–1092. https://doi.org/10.1175/1520-0450(1983)022<1065:BPOTSF>2.0.CO;2

Luckman, A. (2014). Surface melt and ponding on Larsen C Ice Shelf and the impact of föhn winds. Antarctic Science, 26(6), 625.

Marshall, G. J., Orr, A., van Lipzig, N. P. M., & King, J. C. (2006). The Impact of a Changing Southern Hemisphere Annular Mode on Antarctic Peninsula Summer Temperatures. Journal of Climate, 19(20), 5388–5404. https://doi.org/10.1175/JCLI3844.1

Marshall, G. J., Thompson, D. W. J., & Broeke, M. R. van den. (2017). The Signature of Southern Hemisphere Atmospheric Circulation Patterns in Antarctic Precipitation. Geophysical Research Letters, 44(22), 11,580-11,589. https://doi.org/10.1002/2017GL075998

Marshall, Gareth & National Center for Atmospheric Research Staff (Eds). (2018). Last modified 19 Mar 2018. "The Climate Data Guide: Marshall Southern Annular Mode (SAM) Index (Station-based)." Retrieved from https://climatedataguide.ucar.edu/climate-data/marshall-southern-annular-mode-sam-index-station-based.

Matus, A. V., & L'Ecuyer, T. S. (2017). The role of cloud phase in Earth's radiation budget. Journal of Geophysical Research: Atmospheres, 122(5), 2559–2578. https://doi.org/10.1002/2016JD025951

Morcrette, J.-J. (2002). The Surface Downward Longwave Radiation in the ECMWF Forecast System. Journal of Climate, 15(14), 1875–1892. https://doi.org/10.1175/1520-0442(2002)015<1875:TSDLRI>2.0.CO;2

Parish, T. R. (1983). The influence of the Antarctic Peninsula on the wind field over the western Weddell Sea. Journal of Geophysical Research: Oceans, 88(C4), 2684–2692. https://doi.org/10.1029/JC088iC04p02684

Pomeroy, J. W., & Male, D. H. (1992). Steady-state suspension of snow. Journal of Hydrology, 136(1–4), 275–301. https://doi.org/10.1016/0022-1694(92)90015-N

Pritchard, H. D., Arthern, R. J., Vaughan, D. G., & Edwards, L. A. (2009). Extensive dynamic thinning on the margins of the Greenland and Antarctic ice sheets. Nature, 461(7266), 971–975. https://doi.org/10.1038/nature08471

Reijmer, C. H., Broeke, M. R. van den, Fettweis, X., Ettema, J., & Stap, L. B. (2012). Refreezing on the Greenland ice sheet: a comparison of parameterizations. The Cryosphere, 6(4), 743–762. https://doi.org/https://doi.org/10.5194/tc-6-743-2012

Rignot, E., Mouginot, J., Scheuchl, B., Broeke, M. van den, Wessem, M. J. van, & Morlighem, M. (2019). Four decades of Antarctic Ice Sheet mass balance from 1979–2017. Proceedings of the National Academy of Sciences, 116(4), 1095–1103. https://doi.org/10.1073/pnas.1812883116

Schannwell, C., Cornford, S., Pollard, D., & Barrand, N. E. (2018). Dynamic response of Antarctic Peninsula Ice Sheet to potential collapse of Larsen C and George VI ice shelves. The Cryosphere, 12(7), 2307–2326. https://doi.org/https://doi.org/10.5194/tc-12-2307-2018

Schröder, L., Horwath, M., Dietrich, R., Helm, V., Broeke, M. R. van den, & Ligtenberg, S. R. M. (2019). Four decades of Antarctic surface elevation changes from multi-mission satellite altimetry. The Cryosphere, 13(2), 427–449. https://doi.org/https://doi.org/10.5194/tc-13-427-2019

Swart, N. C., Fyfe, J. C., Gillett, N., & Marshall, G. J. (2015). Comparing Trends in the Southern Annular Mode and Surface Westerly Jet. Journal of Climate, 28(22), 8840–8859. https://doi.org/10.1175/JCLI-D-15-0334.1

Thompson, D. W. J., Solomon, S., Kushner, P. J., England, M. H., Grise, K. M., & Karoly, D. J. (2011). Signatures of the Antarctic ozone hole in Southern Hemisphere surface climate change. Nature Geoscience, 4(11), 741–749. https://doi.org/10.1038/ngeo1296

Turner, J., Barrand, N. E., Bracegirdle, T. J., Convey, P., Hodgson, D. A., Jarvis, M., … Klepikov, A. (2014). Antarctic climate change and the environment: an update. Polar Record, 50(3), 237–259. https://doi.org/10.1017/S0032247413000296

Turner, J., Lu, H., White, I., King, J. C., Phillips, T., Hosking, J. S., … Deb, P. (2016). Absence of 21st century warming on Antarctic Peninsula consistent with natural variability. Nature, 535(7612), 411–415. https://doi.org/10.1038/nature18645

Turner, J., Maksym, T., Phillips, T., Marshall, G. J., & Meredith, M. P. (2013). The impact of changes in sea ice advance on the large winter warming on the western Antarctic Peninsula. International Journal of Climatology, 33(4), 852–861. https://doi.org/10.1002/joc.3474

van Lipzig, N. P. M., Marshall, G. J., Orr, A., & King, J. C. (2008). The Relationship between the Southern Hemisphere Annular Mode and Antarctic Peninsula Summer Temperatures: Analysis of a High-Resolution Model Climatology. Journal of Climate, 21(8), 1649–1668. https://doi.org/10.1175/2007JCLI1695.1

van Wessem, J. M., Berg, W. J. van de, Noël, B. P. Y., Meijgaard, E. van, Amory, C., Birnbaum, G., … Broeke, M. R. van den. (2018). Modelling the climate and surface mass

balance of polar ice sheets using RACMO2 – Part 2: Antarctica (1979–2016). The Cryosphere, 12(4), 1479‑1498. https://doi.org/https://doi.org/10.5194/tc-12-1479-2018

van Wessem, J. M., Ligtenberg, S. R. M., Reijmer, C. H., van de Berg, W. J., van den Broeke, M. R., Barrand, N. E., … Meijgaard, E. van. (2016). The modelled surface mass balance of the Antarctic Peninsula at 5.5 km horizontal resolution. The Cryosphere, 10(1), 271‑285. https://doi.org/https://doi.org/10.5194/tc-10-271-2016

van Wessem, J. M., Reijmer, C. H., van de Berg, W. J., van den Broeke, M. R., Cook, A. J., van Ulft, L. H., & van Meijgaard, E. (2015). Temperature and Wind Climate of the Antarctic Peninsula as Simulated by a High-Resolution Regional Atmospheric Climate Model. Journal of Climate, 28(18), 7306‑7326. https://doi.org/10.1175/JCLI-D-15-0060.1

Wyard, C., Scholzen, C., Fettweis, X., Van Campenhout, J., & François, L. (2017). Decrease in climatic conditions favouring floods in the south-east of Belgium over 1959–2010 using the regional climate model MAR. International Journal of Climatology, 37(5), 2782‑2796. https://doi.org/10.1002/joc.4879

Zhang, F. (2002). Vertical resolution and coordinates. Departement of Atmospheric Siences, Texas A&M University. http://www.met.tamu.edu/class/metr452/models/2001/vertres.html. Consulté le 15 juillet 2019.